Analysis of an augmented pseudostress-based mixed formulation for a nonlinear Brinkman model of porous media flow*

Gabriel N. Gatica† Luis F. Gatica‡ Filánder A. Sequeira§

Abstract

In this paper we introduce and analyze an augmented mixed finite element method for the two-dimensional nonlinear Brinkman model of porous media flow with mixed boundary conditions. More precisely, we extend a previous approach for the respective linear model to the present nonlinear case, and employ a dual-mixed formulation in which the main unknowns are given by the gradient of the velocity and the pseudostress. In this way, and similarly as before, the original velocity and pressure unknowns are easily recovered through a simple postprocessing. In addition, since the Neumann boundary condition becomes essential, we impose it in a weak sense, which yields the introduction of the trace of the fluid velocity over the Neumann boundary as the associated Lagrange multiplier. We apply known results from nonlinear functional analysis to prove that the corresponding continuous and discrete schemes are well-posed. In particular, a feasible choice of finite element subspaces is given by Raviart-Thomas elements of order $k \geq 0$ for the pseudostress, piecewise polynomials of degree $\leq k$ for the gradient, and continuous piecewise polynomials of degree $\leq k+1$ for the Lagrange multiplier. We also derive a reliable and efficient residual-based a posteriori error estimator for this problem. Finally, several numerical results illustrating the performance and the robustness of the method, confirming the theoretical properties of the estimator, and showing the behaviour of the associated adaptive algorithm, are provided.

Key words: nonlinear Brinkman model, mixed finite element method, augmented formulation, high-order approximations

1 Introduction

The Brinkman model of porous media flow, which can be seen as a mixture of Darcy's and Stokes' equations, is usually hard to solve, firstly because of the wide range of possible permeability ratios, and secondly due to the nature of the mixed boundary conditions involved. One way of solving the first issue is by means of stabilized methods (see, e.g. [3], [17]), whereas the weak imposition of the Dirichlet boundary conditions, using Nitsche's method, has been applied recently to deal with the second difficulty (see, e.g. [14] and the references therein). However, most of the variational

*This work was partially supported by CONICYT-Chile through BASAL project CMM, Universidad de Chile, project Anillo ACT1118 (ANANUM), and the Becas-Chile Programme for foreign students; by Centro de Investigación en Ingeniería Matemática (CI^{2}MA), Universidad de Concepción; and by Dirección de Investigación of the Universidad Católica de la Santísima Concepción, through the project DIN 07/2014.

†CI^{2}MA and Departamento de Ingeniería Matemática, Universidad de Concepción, Casilla 160-C, Concepción, Chile, email: ggatica@ci2ma.udec.cl.

‡CI^{2}MA - Universidad de Concepción, and Departamento de Matemática y Física Aplicadas, Facultad de Ingeniería, Universidad Católica de la Santísima Concepción, Casilla 297, Concepción, Chile, email: lgatica@ucsc.cl

§Escuela de Matemática, Universidad Nacional de Costa Rica, Heredia, Costa Rica, email: filander.sequeira@una.cr. Present address: CI^{2}MA and Departamento de Ingeniería Matemática, Universidad de Concepción, Casilla 160-C, Concepción, Chile, email: fsequeira@ci2ma.udec.cl.

formulations found in the literature are based on the typical Stokes-type (also called primal-mixed) approach in which the velocity and the pressure are kept as the main unknowns. Actually, up to the authors' knowledge, no stress-based or pseudostress-based approaches seemed to be available until the recent contribution [9], where an alternative way of dealing with the mixed boundary conditions and the a priori and a posteriori error analyses of a dual-mixed approach for the two-dimensional Brinkman problem were provided. Indeed, the pseudostress $\boldsymbol{\sigma}$ is the main unknown of the resulting saddle point problem in [9], and the velocity and pressure are easily recovered in terms of $\boldsymbol{\sigma}$ through simple postprocessing formulae. In addition, as it is usual for dual-mixed methods, the Dirichlet boundary condition for the velocity becomes natural in this case, and the Neumann boundary condition, being essential, is imposed weakly through the introduction of the trace of the velocity on that boundary as the associated Lagrange multiplier. In this way, the Babuška-Brezzi theory is applied first in [9] to establish sufficient conditions for the well-posedness of the resulting continuous and discrete formulations. In particular, a feasible choice of finite element subspaces is given by Raviart-Thomas elements of order $k \geq 0$ for the pseudostress, and continuous piecewise polynomials of degree $k+1$ for the Lagrange multiplier. Next, a reliable and efficient residual-based a posteriori error estimator is derived there. Suitable auxiliary problems, the continuous inf-sup conditions satisfied by the bilinear forms involved, a discrete Helmholtz decomposition, and the local approximation properties of the Raviart-Thomas and Clément interpolation operators are the main tools for proving the reliability. In turn, Helmholtz's decomposition, inverse inequalities, and the localization technique based on triangle-bubble and edge-bubble functions are employed to show the efficiency.

The purpose of the present paper is to extend the analysis and results from [9] to a class of Brinkman models whose viscosity depends nonlinearly on the gradient of the velocity, which is a characteristic feature of quasi-Newtonian Stokes flows (see, e.g. [10, 13, 16]). To this end, we introduce the gradient of the velocity as a new unknown and follow the approach from [13] to deal with the aforedescribed nonlinearity. Moreover, in order to be able to apply the abstract theory from [23] dealing with nonlinear saddle point problems (see also [7], [11]), we need to modify the resulting variational formulation by augmenting it with a redundant equation arising from the constitutive law relating the pseudostress and the velocity gradient. The rest of this work is organized as follows. In Section 2 we define our nonlinear Brinkman model. Then, in Section 3 we introduce the augmented continuous formulation and analize its solvability. The associated mixed finite element method is introduced and analyzed in Section 4. Next, in Section 5 we basically apply the techniques from [6], [12], and [13], to derive a reliable and efficient residual-based a posteriori error estimator for our Galerkin scheme. Finally, some numerical results showing the good performance and robustness of the mixed finite element method, confirming the reliability and efficiency of the estimator, and illustrating the behavior of the associated adaptive algorithm are reported in Section 6.

We end this section with some notations to be used below. Given $\boldsymbol{\tau} := (\tau_{ij})$, $\boldsymbol{\zeta} := (\zeta_{ij}) \in R^{2\times 2}$, we write as usual

$$\boldsymbol{\tau}^{\mathrm{t}} := (\tau_{ji}), \quad \mathrm{tr}\,(\boldsymbol{\tau}) := \sum_{i=1}^{2} \tau_{ii}, \quad \boldsymbol{\tau}^{\mathrm{d}} := \boldsymbol{\tau} - \frac{1}{2}\mathrm{tr}\,(\boldsymbol{\tau})\,\mathbb{I}, \quad \text{and} \quad \boldsymbol{\tau} : \boldsymbol{\zeta} := \sum_{i,j=1}^{2} \tau_{ij}\zeta_{ij},$$

where $\mathbb{I}$ is the identity matrix of $R^{2\times 2}$. In addition, in what follows we utilize standard simplified terminology for Sobolev spaces and norms. In particular, if $\mathcal{O} \subset R^2$ is a domain, $\mathcal{S} \subset R^2$ is a Lipschitz curve, and $r \in R$, we define

$$\mathbf{H}^r(\mathcal{O}) := [H^r(\mathcal{O})]^2, \quad \mathbb{H}^r(\mathcal{O}) := [H^r(\mathcal{O})]^{2\times 2}, \quad \text{and} \quad \mathbf{H}^r(\mathcal{S}) := [H^r(\mathcal{S})]^2.$$

However, when $r = 0$ we usually write $\mathbf{L}^2(\mathcal{O})$, $\mathbb{L}^2(\mathcal{O})$, and $\mathbf{L}^2(\mathcal{S})$ instead of $\mathbf{H}^0(\mathcal{O})$, $\mathbb{H}^0(\mathcal{O})$, and $\mathbf{H}^0(\mathcal{S})$, respectively. The corresponding norms are denoted by $\|\cdot\|_{r,\mathcal{O}}$ [for $H^r(\mathcal{O})$, $\mathbf{H}^r(\mathcal{O})$, and $\mathbb{H}^r(\mathcal{O})$] and $\|\cdot\|_{r,\mathcal{S}}$ [for $H^r(\mathcal{S})$ and $\mathbf{H}^r(\mathcal{S})$]. In general, given any Hilbert space H, we use $\mathbf{H}$ and $\mathbb{H}$ to denote H^2

and $H^{2\times 2}$, respectively. In turn, the Hilbert space

$$\mathbf{H}(\mathrm{div};\mathcal{O}) \;:=\; \left\{\mathbf{w}\in\mathbf{L}^2(\mathcal{O}) \;:\; \mathrm{div}(\mathbf{w})\in L^2(\mathcal{O})\right\},$$

is standard in the realm of mixed problems (see [2]). The space of matrix valued functions whose rows belong to $\mathbf{H}(\mathrm{div};\mathcal{O})$ will be denoted $\mathbb{H}(\mathbf{div};\mathcal{O})$. Hereafter, **div** denotes the usual divergence operator div acting along each row of the corresponding tensor. The Hilbert norms of $\mathbf{H}(\mathrm{div};\mathcal{O})$ and $\mathbb{H}(\mathbf{div};\mathcal{O})$ are denoted by $\|\cdot\|_{\mathrm{div},\mathcal{O}}$ and $\|\cdot\|_{\mathbf{div},\mathcal{O}}$, respectively. Note that if $\boldsymbol{\tau}\in\mathbb{H}(\mathbf{div};\mathcal{O})$, then $\mathbf{div}(\boldsymbol{\tau})\in\mathbf{L}^2(\mathcal{O})$. Finally, we employ $\mathbf{0}$ to denote a generic null vector (including the null functional and operator), and use C and c, with or without subscripts, bars, tildes or hats, to denote generic constants independent of the discretization parameters, which may take different values at different places.

2 The nonlinear Brinkman model

Let Ω be a bounded and simply connected domain in R^2 with polygonal boundary Γ, and such that all its interior angles lie in $(0,2\pi)$. Also, let Γ_D and Γ_N be disjoint open subsets of Γ, with $|\Gamma_D|$, $|\Gamma_N|\neq 0$, such that $\Gamma=\bar{\Gamma}_D\cup\bar{\Gamma}_N$. Then, given $\mathbf{f}\in\mathbf{L}^2(\Omega)$ and $\mathbf{g}\in\mathbf{H}^{-1/2}(\Gamma_N)$, our boundary value problem reads as follows: Find a tensor field $\boldsymbol{\sigma}$ (pseudostress), a vector field $\mathbf{u}$ (velocity), and a scalar field p (pressure) in appropriate spaces such that

$$\begin{array}{rcl} \boldsymbol{\sigma} &=& \mu(|\nabla\mathbf{u}|)\nabla\mathbf{u}-p\mathbb{I} \quad \text{in } \Omega, \quad \alpha\mathbf{u}-\mathbf{div}(\boldsymbol{\sigma}) \;=\; \mathbf{f} \quad \text{in } \Omega,\\ \mathrm{div}(\mathbf{u}) &=& 0 \quad \text{in } \Omega, \quad \mathbf{u} \;=\; \mathbf{0} \quad \text{on } \Gamma_D, \quad \boldsymbol{\sigma}\boldsymbol{\nu} \;=\; \mathbf{g} \quad \text{on } \Gamma_N, \end{array} \tag{2.1}$$

where $\mu: R^+\to R^+$ is the nonlinear dynamic viscosity function, $\alpha>0$ is the viscosity divided by the permeability, $|\cdot|$ is the euclidean norm of $R^{2\times 2}$, and $\boldsymbol{\nu}$ is the unit outward normal to Γ. We recall here that the Sobolev space $\mathbf{H}^{-1/2}(\Gamma_N)$ is defined as the dual of $\mathbf{H}^{1/2}_{00}(\Gamma_N)$, where

$$\mathbf{H}^{1/2}_{00}(\Gamma_N) \;:=\; \left\{\mathbf{v}|_{\Gamma_N} \;:\; \mathbf{v}\in\mathbf{H}^1(\Omega), \quad \mathbf{v}=\mathbf{0} \;\text{ on }\; \Gamma_D\right\}.$$

The corresponding duality pairing with respect to the $\mathbf{L}^2(\Gamma_N)$ - inner product is denoted by $\langle\cdot,\cdot\rangle_{\Gamma_N}$. In addition, throughout the paper $\|\cdot\|_{0;1/2,\Gamma_N}$ stands for the usual norm of both $H^{1/2}_{00}(\Gamma_N)$ and $\mathbf{H}^{1/2}_{00}(\Gamma_N)$ (see [9]) .

On the other hand, in what follows we let $\psi_{ij}: R^{2\times 2}\to R$ be the mapping given by $\psi_{ij}(\mathbf{r}):=\mu(|\mathbf{r}|)r_{ij}$ for all $\mathbf{r}:=(r_{ij})\in R^{2\times 2}$, for all $i,j\in\{1,2\}$. Then, throughout this paper we assume that μ is of class C^1 and that there exist $\gamma_0,\alpha_0>0$ such that for all $\mathbf{r}:=(r_{ij})$, $\mathbf{s}:=(s_{ij})\in R^{2\times 2}$, there holds

$$|\psi_{ij}(\mathbf{r})| \;\leq\; \gamma_0\|\mathbf{r}\|_{R^{2\times 2}}, \qquad \left|\frac{\partial}{\partial r_{kl}}\psi_{ij}(\mathbf{r})\right| \;\leq\; \gamma_0, \quad \forall\; i,j,k,l\in\{1,2\}, \tag{2.2}$$

and

$$\sum_{i,j,k,l=1}^{2}\frac{\partial}{\partial r_{kl}}\psi_{ij}(\mathbf{r})s_{ij}s_{kl} \;\geq\; \alpha_0\|\mathbf{s}\|^2_{R^{2\times 2}}. \tag{2.3}$$

For example, the Carreau law for viscoplastic flows (see, e.g. [18, 22]), given by

$$\mu(t):=\mu_0+\mu_1(1+t^2)^{(\beta-2)/2} \quad \forall\; t\in R^+,$$

satisfies (2.2) and (2.3) for all $\mu_0,\mu_1>0$, and for all $\beta\in[1,2]$. In particular, note that with $\beta=2$ we recover the usual linear Brinkman model.

Now, we observe that the pair of equations given by

$$\boldsymbol{\sigma} \;=\; \mu(|\nabla \mathbf{u}|)\nabla \mathbf{u} - p\mathbb{I} \quad \text{in } \Omega, \quad \text{and} \quad \mathrm{div}(\mathbf{u}) \;=\; 0 \quad \text{in } \Omega,$$

is equivalent to

$$\boldsymbol{\sigma} \;=\; \mu(|\nabla \mathbf{u}|)\nabla \mathbf{u} - p\mathbb{I} \quad \text{in } \Omega, \quad \text{and} \quad p \;=\; -\frac{1}{2}\,\mathrm{tr}\,(\boldsymbol{\sigma}) \quad \text{in } \Omega, \tag{2.4}$$

whence introducing the gradient $\mathbf{t} := \nabla \mathbf{u}$ in Ω, as an auxiliary unknown, we can rewrite (2.1) as follows

$$\begin{array}{l} \mathbf{t} \;=\; \nabla \mathbf{u} \quad \text{in } \Omega, \quad \boldsymbol{\sigma}^{\mathrm{d}} \;=\; \boldsymbol{\psi}(\mathbf{t}) \quad \text{in } \Omega, \quad \alpha \mathbf{u} - \mathbf{div}(\boldsymbol{\sigma}) \;=\; \mathbf{f} \quad \text{in } \Omega, \\ \mathrm{tr}\,(\mathbf{t}) \;=\; 0 \quad \text{in } \Omega, \quad \mathbf{u} \;=\; \mathbf{0} \quad \text{on } \Gamma_D, \quad \boldsymbol{\sigma}\boldsymbol{\nu} \;=\; \mathbf{g} \quad \text{on } \Gamma_N, \end{array} \tag{2.5}$$

where $\boldsymbol{\psi} : R^{2\times 2} \to R^{2\times 2}$ is given by $\boldsymbol{\psi}(\mathbf{r}) := (\psi_{ij}(\mathbf{r})) = (\mu(|\mathbf{r}|)r_{ij})$ for all $\mathbf{r} := (r_{ij}) \in R^{2\times 2}$.

3 The continuous formulation

3.1 The augmented approach

Initially we test the first and second equations of (2.5) with $\boldsymbol{\tau} \in \mathbb{H}(\mathbf{div};\Omega)$ and $\mathbf{s} \in \mathbb{L}^2_{\mathrm{tr}}(\Omega)$, respectively, where

$$\mathbb{L}^2_{\mathrm{tr}}(\Omega) \;:=\; \left\{ \mathbf{s} \in \mathbb{L}^2(\Omega) \;:\; \mathrm{tr}\,(\mathbf{s}) \;=\; 0 \right\}.$$

Then, integrating by parts the expression $\int_\Omega \nabla \mathbf{u} : \boldsymbol{\tau}$, using the Dirichlet boundary condition, recalling that $\mathrm{tr}\,(\mathbf{t}) \;=\; 0$, and introducing the auxiliary unknown $\boldsymbol{\xi} := -\mathbf{u}|_{\Gamma_N} \in \mathbf{H}^{1/2}_{00}(\Gamma_N)$, we arrive at

$$\begin{array}{rcl} \displaystyle\int_\Omega \boldsymbol{\psi}(\mathbf{t}) : \mathbf{s} - \int_\Omega \mathbf{s} : \boldsymbol{\sigma}^{\mathrm{d}} & = & 0 \quad \forall\, \mathbf{s} \in \mathbb{L}^2_{\mathrm{tr}}(\Omega), \\ \displaystyle\int_\Omega \mathbf{t} : \boldsymbol{\tau}^{\mathrm{d}} + \int_\Omega \mathbf{u} \cdot \mathbf{div}(\boldsymbol{\tau}) + \langle \boldsymbol{\tau}\boldsymbol{\nu}, \boldsymbol{\xi} \rangle_{\Gamma_N} & = & 0 \quad \forall\, \boldsymbol{\tau} \in \mathbb{H}(\mathbf{div};\Omega). \end{array} \tag{3.6}$$

In turn, the Neumann boundary condition is imposed weakly as

$$\langle \boldsymbol{\sigma}\boldsymbol{\nu}, \boldsymbol{\lambda} \rangle_{\Gamma_N} \;=\; \langle \mathbf{g}, \boldsymbol{\lambda} \rangle_{\Gamma_N} \quad \forall\, \boldsymbol{\lambda} \in \mathbf{H}^{1/2}_{00}(\Gamma_N),$$

and replacing $\mathbf{u}$ in (3.6) by

$$\mathbf{u} \;=\; \frac{1}{\alpha}\left\{ \mathbf{f} \;+\; \mathbf{div}(\boldsymbol{\sigma}) \right\} \quad \text{in } \Omega, \tag{3.7}$$

we obtain that

$$\int_\Omega \mathbf{t} : \boldsymbol{\tau}^{\mathrm{d}} + \frac{1}{\alpha}\int_\Omega \mathbf{div}(\boldsymbol{\sigma}) \cdot \mathbf{div}(\boldsymbol{\tau}) + \langle \boldsymbol{\tau}\boldsymbol{\nu}, \boldsymbol{\xi} \rangle_{\Gamma_N} \;=\; -\frac{1}{\alpha}\int_\Omega \mathbf{f} \cdot \mathbf{div}(\boldsymbol{\tau}) \quad \forall\, \boldsymbol{\tau} \in \mathbb{H}(\mathbf{div};\Omega).$$

Finally, for sake of feasibility of the forthcoming analysis, namely to be able to apply the abstract theory from [23], we enrich the foregoing equations with the introduction of the constitutive law relating $\boldsymbol{\sigma}$ and $\mathbf{t}$ (written as in the second equation of (2.5)) multiplied by a stabilization parameter. More precisely, given $\kappa > 0$, to be chosen later, we add

$$\kappa \int_\Omega \left(\boldsymbol{\sigma}^{\mathrm{d}} - \boldsymbol{\psi}(\mathbf{t}) \right) : \boldsymbol{\tau}^{\mathrm{d}} \;=\; 0 \quad \forall\, \boldsymbol{\tau} \in \mathbb{H}(\mathbf{div};\Omega), \tag{3.8}$$

and then, we obtain the variational formulation: Find $((\mathbf{t},\boldsymbol{\sigma}),\boldsymbol{\xi}) \in H \times Q$ such that

$$\begin{array}{rcll} [\mathcal{A}(\mathbf{t},\boldsymbol{\sigma}),(\mathbf{s},\boldsymbol{\tau})] \ + \ [\mathcal{B}(\mathbf{s},\boldsymbol{\tau}),\boldsymbol{\xi}] & = & [\mathcal{F},(\mathbf{s},\boldsymbol{\tau})] & \forall\ (\mathbf{s},\boldsymbol{\tau}) \in H, \\ [\mathcal{B}(\mathbf{t},\boldsymbol{\sigma}),\boldsymbol{\lambda}] & = & [\mathcal{G},\boldsymbol{\lambda}] & \forall\ \boldsymbol{\lambda} \in Q, \end{array} \tag{3.9}$$

where $H := \mathbb{L}^2_{\rm tr}(\Omega) \times \mathbb{H}(\mathbf{div};\Omega)$, $Q := \mathbf{H}^{1/2}_{00}(\Gamma_N)$, and the nonlinear operator $\mathcal{A} : H \to H'$, the linear operator $\mathcal{B} : H \to Q'$, and the functionals $\mathcal{F} \in H'$ and $\mathcal{G} \in Q'$, are defined by

$$\begin{aligned} [\mathcal{A}(\mathbf{t},\boldsymbol{\sigma}),(\mathbf{s},\boldsymbol{\tau})] \ := \ & \int_\Omega \boldsymbol{\psi}(\mathbf{t}) : \mathbf{s} \ - \ \int_\Omega \mathbf{s} : \boldsymbol{\sigma}^{\rm d} + \int_\Omega \mathbf{t} : \boldsymbol{\tau}^{\rm d} \\ & + \kappa \int_\Omega \Big(\boldsymbol{\sigma}^{\rm d} \ - \ \boldsymbol{\psi}(\mathbf{t}) \Big) : \boldsymbol{\tau}^{\rm d} + \frac{1}{\alpha} \int_\Omega \mathbf{div}(\boldsymbol{\sigma}) \cdot \mathbf{div}(\boldsymbol{\tau}) \, , \end{aligned} \tag{3.10}$$

$$[\mathcal{B}(\mathbf{s},\boldsymbol{\tau}),\boldsymbol{\lambda}] \ := \ \langle \boldsymbol{\tau}\boldsymbol{\nu}, \boldsymbol{\lambda} \rangle_{\Gamma_N} \ , \tag{3.11}$$

$$[\mathcal{F},(\mathbf{s},\boldsymbol{\tau})] \ := \ -\frac{1}{\alpha} \int_\Omega \mathbf{f} \cdot \mathbf{div}(\boldsymbol{\tau}) \, ,$$

$$[\mathcal{G},\boldsymbol{\lambda}] \ := \ \langle \mathbf{g}, \boldsymbol{\lambda} \rangle_{\Gamma_N} \ , \tag{3.12}$$

where $[\cdot,\cdot]$ stands in each case for the duality pairing induced by the corresponding operators and functionals.

3.2 Analysis of the augmented formulation

The purpose of this section is to establish the well-posedness of (3.9). We begin the analysis by recalling from [23] the following abstract theorem.

Theorem 3.1. *Let X and M be Hilbert spaces, and let $\mathcal{A} : X \to X'$ and $\mathcal{B} : X \to M'$ be nonlinear and linear operators, respectively. Let $V := Ker(\mathcal{B}) = \{x \in X : [\mathcal{B}(x), q] = 0 \ \forall q \in M\}$. Assume that $\mathcal{A}$ is Lipschitz-continuous on X and that for all $\widetilde{z} \in X$, $\mathcal{A}(\widetilde{z} + \cdot\ )$ is uniformly strongly monotone on V, that is, there exist constants c_1, $c_2 > 0$ such that*

$$\|\mathcal{A}(x) - \mathcal{A}(y)\|_{X'} \ \leq \ c_1 \|x - y\|_X \quad \forall\ x, y \in X,$$

and

$$[\mathcal{A}(\widetilde{z} + x) - \mathcal{A}(\widetilde{z} + y)] \ \geq \ c_2 \|x - y\|^2_X,$$

for all $\widetilde{z} \in X$ and for all $x, y \in V$. In addition, assume that there exists $\beta > 0$ such that for all $q \in M$

$$\sup_{\substack{x \in X \\ x \neq \mathbf{0}}} \frac{[\mathcal{B}(x), q]}{\|x\|_X} \ \geq \ \beta \|q\|_M.$$

Then, given $(\mathcal{F},\mathcal{G}) \in X' \times M'$, there exists a unique $(x, p) \in X \times M$ such that

$$\begin{array}{rcll} [\mathcal{A}(x), y] \ + \ [\mathcal{B}(y), p] & = & [\mathcal{F}, y] & \forall\ y \in X, \\ [\mathcal{B}(x), q] & = & [\mathcal{G}, q] & \forall\ q \in M. \end{array}$$

Further, the following estimates hold

$$\|x\|_X \ \leq \ \frac{1}{c_2} \|\mathcal{F}\| + \frac{1}{\beta} \left(1 + \frac{c_1}{c_2} \right) \|\mathcal{G}\|, \tag{3.13}$$

$$\|p\|_M \ \leq \ \frac{1}{\beta} \left(1 + \frac{c_1}{c_2} \right) \left(\|\mathcal{F}\| + \frac{c_1}{\beta} \|\mathcal{G}\| \right). \tag{3.14}$$

Proof. See [23, Proposition 2.3] or [13, Theorem 3.1]. □

In what follows we apply Theorem 3.1 to the augmented formulation (3.9). The inf-sup condition for the linear operator $\mathcal{B}$ is proved first.

Lemma 3.1. *There exists a positive constant β, depending only on Ω, such that*

$$\sup_{\substack{(\mathbf{s},\boldsymbol{\tau})\in H\\(\mathbf{s},\boldsymbol{\tau})\neq\mathbf{0}}} \frac{[\mathcal{B}(\mathbf{s},\boldsymbol{\tau}),\boldsymbol{\lambda}]}{\|(\mathbf{s},\boldsymbol{\tau})\|_H} \;\geq\; \beta\|\boldsymbol{\lambda}\|_{0;1/2,\Gamma_N} \quad \forall\, \boldsymbol{\lambda}\in Q.$$

Proof. Note that $\mathcal{B}: H\to Q'$ is given by $\mathcal{B}(\mathbf{s},\boldsymbol{\tau}) := \boldsymbol{\tau}\boldsymbol{\nu}|_{\Gamma_N} \in \mathbf{H}^{-1/2}(\Gamma_N) = Q' \quad \forall\,(\mathbf{s},\boldsymbol{\tau})\in H$, and hence the fact that the normal trace operator $\gamma_{\boldsymbol{\nu}}: \mathbb{H}(\mathbf{div};\Omega)\to \mathbf{H}^{-1/2}(\Gamma_N)$ is surjective implies the same property for $\mathcal{B}$. □

Next, in order to verify the assumptions required by Theorem 3.1 for our nonlinear operator $\mathcal{A}$, we define the auxiliary nonlinear operator $\mathbb{A}: \mathbb{L}^2_{\rm tr}(\Omega)\to[\mathbb{L}^2_{\rm tr}(\Omega)]'$ given by

$$[\mathbb{A}(\mathbf{r}),\mathbf{s}] \;:=\; \int_\Omega \boldsymbol{\psi}(\mathbf{r}):\mathbf{s} \quad \forall\, \mathbf{r},\mathbf{s}\in\mathbb{L}^2_{\rm tr}(\Omega)\,. \tag{3.15}$$

It is easy to show from (2.2) and (2.3) (see e.g. [13, Lemma 2.1]) that $\mathbb{A}$ is Lipschitz-continuous and strongly monotone.

Lemma 3.2. *Let γ_0 and α_0 be the constants of* (2.2) *and* (2.3)*, respectively. Then, for each $\mathbf{r},\mathbf{s}\in\mathbb{L}^2_{\rm tr}(\Omega)$ there hold*

$$\|\mathbb{A}(\mathbf{r})-\mathbb{A}(\mathbf{s})\|_{[\mathbb{L}^2(\Omega)]'} \;\leq\; \gamma_0\|\mathbf{r}-\mathbf{s}\|_{0,\Omega}, \tag{3.16}$$

and

$$[\mathbb{A}(\mathbf{r})-\mathbb{A}(\mathbf{s}),\mathbf{r}-\mathbf{s}] \;\geq\; \alpha_0\|\mathbf{r}-\mathbf{s}\|^2_{0,\Omega}. \tag{3.17}$$

Proof. It suffices to observe that for each $\widetilde{\mathbf{r}}\in\mathbb{L}^2_{\rm tr}(\Omega)$ the Gâteuax derivative $\mathcal{D}\mathbb{A}(\widetilde{\mathbf{r}})$ is a bilinear form on $\mathbb{L}^2_{\rm tr}(\Omega)\times\mathbb{L}^2_{\rm tr}(\Omega)$, which is uniformly bounded and uniformly $\mathbb{L}^2_{\rm tr}(\Omega)$-elliptic (see [13, Lemma 2.1] for details). □

We are now ready to establish that the nonlinear operator $\mathcal{A}$ (cf. (3.10)) is also Lipschitz-continuous on H.

Lemma 3.3. *Let $\mathcal{A}$ be the nonlinear operator defined in* (3.10)*. Then, there exists a constant $C_{\rm LC}>0$ such that*

$$\|\mathcal{A}(\mathbf{t},\boldsymbol{\sigma})-\mathcal{A}(\mathbf{s},\boldsymbol{\tau})\|_{H'} \;\leq\; C_{\rm LC}\|(\mathbf{t},\boldsymbol{\sigma})-(\mathbf{s},\boldsymbol{\tau})\|_H \quad \forall\,(\mathbf{t},\boldsymbol{\sigma}),(\mathbf{s},\boldsymbol{\tau})\in H.$$

Proof. Given $(\mathbf{t},\boldsymbol{\sigma}),(\mathbf{s},\boldsymbol{\tau})$ and $(\mathbf{r},\boldsymbol{\rho})\in H$, we obtain, according to the definition of $\mathcal{A}$ and $\mathbb{A}$, that

$$\begin{aligned}[\mathcal{A}(\mathbf{t},\boldsymbol{\sigma})-\mathcal{A}(\mathbf{s},\boldsymbol{\tau}),(\mathbf{r},\boldsymbol{\rho})] \;=\; [\mathbb{A}(\mathbf{t})-\mathbb{A}(\mathbf{s}),\mathbf{r}] \;-\; \kappa[\mathbb{A}(\mathbf{t})-\mathbb{A}(\mathbf{s}),\boldsymbol{\rho}^{\rm d}] \;-\; \int_\Omega \mathbf{r}:(\boldsymbol{\sigma}-\boldsymbol{\tau})^{\rm d}\\ +\quad \int_\Omega(\mathbf{t}-\mathbf{s}):\boldsymbol{\rho}^{\rm d} \;+\; \kappa\int_\Omega(\boldsymbol{\sigma}-\boldsymbol{\tau})^{\rm d}:\boldsymbol{\rho}^{\rm d} + \frac{1}{\alpha}\int_\Omega \mathbf{div}(\boldsymbol{\sigma}-\boldsymbol{\tau})\cdot\mathbf{div}(\boldsymbol{\rho})\,.\end{aligned} \tag{3.18}$$

Hence, it follows easily from (3.18), (3.16), and the Cauchy-Schwarz inequality, that $\mathcal{A}$ is Lipschitz-continuous on H with the constant $C_{\rm LC} := 3\max\{1,\gamma_0,\kappa,\kappa\gamma_0,\alpha^{-1}\}$. □

Our next goal is to show that for all $(\mathbf{r},\boldsymbol{\rho})\in H$, $\mathcal{A}((\mathbf{r},\boldsymbol{\rho})+\,\cdot\,)$ is uniformly strongly monotone on the kernel of $\mathcal{B}$, given by $V:=\{(\mathbf{s},\boldsymbol{\tau})\in H\ :\ \boldsymbol{\tau}\boldsymbol{\nu}\ =\ \mathbf{0}\ \text{ on }\Gamma_N\}$. To this end, we first consider the decomposition

$$\mathbb{H}(\mathbf{div};\Omega)\ =\ \mathbb{H}_0(\mathbf{div};\Omega)\oplus R\mathbb{I},$$

where $\mathbb{H}_0(\mathbf{div};\Omega):=\{\boldsymbol{\tau}\in\mathbb{H}(\mathbf{div};\Omega)\ :\ \int_\Omega \mathrm{tr}\,(\boldsymbol{\tau})=0\}$. This means that for any $\boldsymbol{\tau}\in\mathbb{H}(\mathbf{div};\Omega)$ there exist unique $\boldsymbol{\tau}_0\in\mathbb{H}_0(\mathbf{div};\Omega)$ and $d:=\frac{1}{2|\Omega|}\int_\Omega \mathrm{tr}\,(\boldsymbol{\tau})\in R$ such that $\boldsymbol{\tau}=\boldsymbol{\tau}_0+d\mathbb{I}$, whence $\|\boldsymbol{\tau}\|^2_{\mathbf{div},\Omega}=\|\boldsymbol{\tau}_0\|^2_{\mathbf{div},\Omega}+2d^2|\Omega|$. In addition, we have the following lemmas.

Lemma 3.4. *There exists $C_1>0$, depending only on Ω, such that*

$$C_1\|\boldsymbol{\tau}_0\|^2_{0,\Omega}\ \leq\ \|\boldsymbol{\tau}^{\mathrm{d}}\|^2_{0,\Omega}\ +\ \|\mathbf{div}(\boldsymbol{\tau})\|^2_{0,\Omega}\quad\forall\,\boldsymbol{\tau}\in\mathbb{H}(\mathbf{div};\Omega).$$

Proof. See [1, Lemma 3.1] or [2, Proposition 3.1, Chapter IV]. □

Lemma 3.5. *There exists $C_2>0$, depending only on Γ_N and Ω, such that*

$$C_2\|\boldsymbol{\tau}\|^2_{\mathbf{div},\Omega}\ \leq\ \|\boldsymbol{\tau}_0\|^2_{\mathbf{div},\Omega}\quad\forall\,\boldsymbol{\tau}\in\mathbb{H}(\mathbf{div};\Omega)\quad\textit{such that}\quad\boldsymbol{\tau}\boldsymbol{\nu}\ =\ \mathbf{0}\quad\textit{on}\quad\Gamma_N.$$

Proof. See [8, Lemma 2.2]. □

The uniform strong monotonicity of $\mathcal{A}((\mathbf{r},\boldsymbol{\rho})+\,\cdot\,)$ on V, for all $(\mathbf{r},\boldsymbol{\rho})\in H$, is proved as follows.

Lemma 3.6. *Let $\mathcal{A}$ and $\mathcal{B}$ be the operators defined in* (3.10) *and* (3.11)*, respectively, and let V be the kernel of $\mathcal{B}$. Assume that the parameter κ lies in $\left(0,\frac{2\alpha_0\delta}{\gamma_0}\right)$ for each $\delta\in\left(0,\frac{2}{\gamma_0}\right)$, where α_0 and γ_0 are the positive constants from* (2.2) *and* (2.3)*. Then, there exists a constant $C_{\mathrm{SM}}>0$ such that for all $(\mathbf{r},\boldsymbol{\rho})\in H$, and for all $(\mathbf{t},\boldsymbol{\sigma}),(\mathbf{s},\boldsymbol{\tau})\in V$ there holds*

$$[\mathcal{A}((\mathbf{r},\boldsymbol{\rho})+(\mathbf{t},\boldsymbol{\sigma}))-\mathcal{A}((\mathbf{r},\boldsymbol{\rho})+(\mathbf{s},\boldsymbol{\tau})),(\mathbf{t},\boldsymbol{\sigma})-(\mathbf{s},\boldsymbol{\tau})]\ \geq\ C_{\mathrm{SM}}\|(\mathbf{t},\boldsymbol{\sigma})-(\mathbf{s},\boldsymbol{\tau})\|^2_H\,.$$

Proof. Given $(\mathbf{r},\boldsymbol{\rho})\in H$ and $(\mathbf{t},\boldsymbol{\sigma}),(\mathbf{s},\boldsymbol{\tau})\in V$, we obtain from (3.18) that

$$\begin{aligned}&[\mathcal{A}((\mathbf{r},\boldsymbol{\rho})+(\mathbf{t},\boldsymbol{\sigma}))-\mathcal{A}((\mathbf{r},\boldsymbol{\rho})+(\mathbf{s},\boldsymbol{\tau})),(\mathbf{t},\boldsymbol{\sigma})-(\mathbf{s},\boldsymbol{\tau})]\\&\quad=\ [\mathbb{A}(\mathbf{r}+\mathbf{t})-\mathbb{A}(\mathbf{r}+\mathbf{s}),\mathbf{t}-\mathbf{s}]-\kappa[\mathbb{A}(\mathbf{r}+\mathbf{t})-\mathbb{A}(\mathbf{r}+\mathbf{s}),(\boldsymbol{\sigma}-\boldsymbol{\tau})^{\mathrm{d}}]\\&\qquad+\ \kappa\|(\boldsymbol{\sigma}-\boldsymbol{\tau})^{\mathrm{d}}\|^2_{0,\Omega}+\frac{1}{\alpha}\|\mathbf{div}(\boldsymbol{\sigma}-\boldsymbol{\tau})\|^2_{0,\Omega}.\end{aligned}$$

Then, using that $[\mathbb{A}(\mathbf{r}+\mathbf{t})-\mathbb{A}(\mathbf{r}+\mathbf{s}),\mathbf{t}-\mathbf{s}]=[\mathbb{A}(\mathbf{r}+\mathbf{t})-\mathbb{A}(\mathbf{r}+\mathbf{s}),(\mathbf{r}+\mathbf{t})-(\mathbf{r}+\mathbf{s})]$, and applying the strong monotonicity and Lipschitz-continuity of $\mathbb{A}$ (cf. Lemma 3.2), we deduce from the foregoing equation that

$$\begin{aligned}&[\mathcal{A}((\mathbf{r},\boldsymbol{\rho})+(\mathbf{t},\boldsymbol{\sigma}))-\mathcal{A}((\mathbf{r},\boldsymbol{\rho})+(\mathbf{s},\boldsymbol{\tau})),(\mathbf{t},\boldsymbol{\sigma})-(\mathbf{s},\boldsymbol{\tau})]\\&\geq\ \alpha_0\|\mathbf{t}-\mathbf{s}\|^2_{0,\Omega}-\kappa\gamma_0\|\mathbf{t}-\mathbf{s}\|_{0,\Omega}\|(\boldsymbol{\sigma}-\boldsymbol{\tau})^{\mathrm{d}}\|_{0,\Omega}+\kappa\|(\boldsymbol{\sigma}-\boldsymbol{\tau})^{\mathrm{d}}\|^2_{0,\Omega}+\frac{1}{\alpha}\|\mathbf{div}(\boldsymbol{\sigma}-\boldsymbol{\tau})\|^2_{0,\Omega}\\&\geq\ \alpha_0\|\mathbf{t}-\mathbf{s}\|^2_{0,\Omega}-\kappa\gamma_0\left\{\frac{\|\mathbf{t}-\mathbf{s}\|^2_{0,\Omega}}{2\delta}+\frac{\delta\|(\boldsymbol{\sigma}-\boldsymbol{\tau})^{\mathrm{d}}\|^2_{0,\Omega}}{2}\right\}+\kappa\|(\boldsymbol{\sigma}-\boldsymbol{\tau})^{\mathrm{d}}\|^2_{0,\Omega}\ +\ \frac{1}{\alpha}\|\mathbf{div}(\boldsymbol{\sigma}-\boldsymbol{\tau})\|^2_{0,\Omega}\\&=\ \left(\alpha_0-\frac{\kappa\gamma_0}{2\delta}\right)\|\mathbf{t}-\mathbf{s}\|^2_{0,\Omega}+\kappa\left(1-\frac{\gamma_0\delta}{2}\right)\|(\boldsymbol{\sigma}-\boldsymbol{\tau})^{\mathrm{d}}\|^2_{0,\Omega}+\frac{1}{\alpha}\|\mathbf{div}(\boldsymbol{\sigma}-\boldsymbol{\tau})\|^2_{0,\Omega}\,,\end{aligned}$$

for all $\delta>0$. It follows that the constants multiplying the norms above become positive if $\delta\in\left(0,\frac{2}{\gamma_0}\right)$ and $\kappa\in\left(0,\frac{2\alpha_0\delta}{\gamma_0}\right)$. Then, applying Lemmas 3.4 and 3.5, we deduce that

$$
\begin{aligned}
&[\mathcal{A}((\mathbf{r},\boldsymbol{\rho})+(\mathbf{t},\boldsymbol{\sigma}))-\mathcal{A}((\mathbf{r},\boldsymbol{\rho})+(\mathbf{s},\boldsymbol{\tau})),(\mathbf{t},\boldsymbol{\sigma})-(\mathbf{s},\boldsymbol{\tau})]\\
&\quad\geq\ \left(\alpha_0-\frac{\kappa\gamma_0}{2\delta}\right)\|\mathbf{t}-\mathbf{s}\|^2_{0,\Omega}+\beta_1\|(\boldsymbol{\sigma}-\boldsymbol{\tau})_0\|^2_{0,\Omega}+\frac{1}{2\alpha}\|\mathbf{div}((\boldsymbol{\sigma}-\boldsymbol{\tau})_0)\|^2_{0,\Omega}\\
&\quad\geq\ \left(\alpha_0-\frac{\kappa\gamma_0}{2\delta}\right)\|\mathbf{t}-\mathbf{s}\|^2_{0,\Omega}+\beta_2\|(\boldsymbol{\sigma}-\boldsymbol{\tau})_0\|^2_{\mathbf{div},\Omega}\\
&\quad\geq\ \left(\alpha_0-\frac{\kappa\gamma_0}{2\delta}\right)\|\mathbf{t}-\mathbf{s}\|^2_{0,\Omega}+C_2\beta_2\|(\boldsymbol{\sigma}-\boldsymbol{\tau})\|^2_{\mathbf{div},\Omega},
\end{aligned}
$$

where $\beta_1 := C_1 \min\left\{1-\frac{\gamma_0\delta}{2},\frac{1}{2\alpha}\right\}>0$ and $\beta_2 := \min\left\{\beta_1,\frac{1}{2\alpha}\right\}>0$. Finally, the proof is completed by choosing $C_{\rm SM} := \min\left\{\alpha_0-\frac{\kappa\gamma_0}{2\delta}, C_2\beta_2\right\}$. □

We remark here that the optimal choice of the stabilization parameter κ, that is the one yielding the largest value of the strong monotonicity constant $C_{\rm SM}$, arises by taking $\delta=\frac{1}{\gamma_0}$ and $\kappa=\frac{\alpha_0}{\gamma_0^2}$.

The well-posedness of our variational formulation (3.9) is provided by the following theorem.

Theorem 3.2. *Assume that* $\mathbf{f}\in\mathbf{L}^2(\Omega)$, $\mathbf{g}\in\mathbf{H}^{-1/2}(\Gamma_N)$, *and that the parameter* κ *lies in* $\left(0,\frac{2\alpha_0\delta}{\gamma_0}\right)$ *for each* $\delta\in\left(0,\frac{2}{\gamma_0}\right)$, *where* α_0 *and* γ_0 *are the positive constants from* (2.2) *and* (2.3). *Then, there exists a unique* $((\mathbf{t},\boldsymbol{\sigma}),\boldsymbol{\xi})\in H\times Q$ *solution of* (3.9). *In addition, there exists a positive constant* C, *depending on* Γ_N, Ω, β, α_0, γ_0, κ, *and* α, *such that*

$$
\|\mathbf{t}\|_{0,\Omega}\ +\ \|\boldsymbol{\sigma}\|_{\mathbf{div},\Omega}\ +\ \|\boldsymbol{\xi}\|_{0;1/2,\Gamma_N}\ \leq\ C\left\{\|\mathbf{f}\|_{0,\Omega}\ +\ \|\mathbf{g}\|_{-1/2,\Gamma_N}\right\}. \tag{3.19}
$$

Proof. Thanks to Lemmas 3.1, 3.3, and 3.6, the proof is a direct application of Theorem 3.1. □

4 The mixed finite element method

In this section we adapt the approach from [9] and define explicit finite element subspaces H_h of $\mathbb{L}^2_{\rm tr}(\Omega)\times\mathbb{H}(\mathbf{div};\Omega)$ and Q_h of $\mathbf{H}^{1/2}_{00}(\Gamma_N)$ such that the mixed finite element scheme associated with the continuous formulation (3.9) is well-posed. For this purpose, let $\{\mathcal{T}_h\}_{h>0}$ be a shape-regular family of triangulations of the polygonal region $\bar\Omega$ by triangles T of diameter h_T, with mesh size $h:=\max\{h_T : T\in\mathcal{T}_h\}$, and such that all the points in $\bar\Gamma_D\cap\bar\Gamma_N$ become vertices of $\mathcal{T}_h$ for all $h>0$. Also, given an integer $k\geq 0$ and a subset S of R^2, we denote by $P_k(S)$ the space of polynomials defined in S of total degree at most k. Then, for each integer $k\geq 0$ and for each $T\in\mathcal{T}_h$, we define the local Raviart-Thomas space of order k (see, e.g. [2], [21])

$$
{\rm RT}_k(T)\ :=\ \mathbf{P}_k(T)\ \oplus\ P_k(T)\mathbf{x},
$$

where $\mathbf{x}=\left(\begin{smallmatrix}x_1\\x_2\end{smallmatrix}\right)$ is a generic vector of R^2, and $\mathbf{P}_k(T):=[P_k(T)]^2$. Now, let $\mathbb{RT}_k(\mathcal{T}_h)$ be the corresponding global Raviart-Thomas tensor space of order k, that is,

$$
\mathbb{RT}_k(\mathcal{T}_h)\ :=\ \left\{\boldsymbol{\tau}\in\mathbb{H}(\mathbf{div};\Omega)\ :\ (\tau_{i1},\tau_{i2})^{\rm t}|_T\in{\rm RT}_k(T)\ \ \forall\ i\in\{1,2\},\quad \forall\ T\in\mathcal{T}_h\right\}.
$$

We also let $\mathbb{X}_h$ be the global tensor space of piecewise polynomials of degree $\leq k$ with zero trace, that is

$$
\mathbb{X}_h\ :=\ \left\{\mathbf{s}\in\mathbb{L}^2_{\rm tr}(\Omega)\ :\ \mathbf{s}|_T\in\mathbb{P}_k(T)\quad\forall\ T\in\mathcal{T}_h\right\},
$$

so that the corresponding finite element subspace H_h for $(\mathbf{t},\boldsymbol{\sigma})\in\mathbb{L}^2_{\rm tr}(\Omega)\times\mathbb{H}(\mathbf{div};\Omega)$ is given by

$$
H_h\ :=\ \mathbb{X}_h\times\mathbb{RT}_k(\mathcal{T}_h). \tag{4.1}
$$

In turn, an eventual finite element subspace for the fluid velocity $\mathbf{u}$ would be given by the global vector space of piecewise polynomials of degree $\leq k$, that is

$$\mathcal{Q}_h^{\mathbf{u}} \;:=\; \left\{ \mathbf{v} \in \mathbf{L}^2(\Omega) \;:\; \mathbf{v}|_T \in \mathbf{P}_k(T) \quad \forall\, T \in \mathcal{T}_h \right\} . \tag{4.2}$$

Next, let Σ_h be the partition on Γ_N induced by the triangulation $\mathcal{T}_h$, and define the mesh size $h_\Sigma := \max\{|e| : e \in \Sigma_h\}$. Then, proceeding exactly as in [9], we consider in what follows two possible choices for Q_h, the finite element subspace approximating the unknown $\boldsymbol{\xi} \in \mathbf{H}_{00}^{1/2}(\Gamma_N)$.

A first choice for Q_h: Let $\Sigma_{\tilde{h}}$ be another partition of Γ_N, completely independent from Σ_h, with $\tilde{h} := \max\{|e| : e \in \Sigma_{\tilde{h}}\}$. Then, given an integer $k \geq 0$, we define

$$Q_h \;:=\; \left\{ \boldsymbol{\lambda}_{\tilde{h}} \in \mathbf{H}_{00}^{1/2}(\Gamma_N) \;:\; \boldsymbol{\lambda}_{\tilde{h}}|_e \in \mathbf{P}_{k+1}(e) \quad \forall\, e \in \Sigma_{\tilde{h}} \right\} . \tag{4.3}$$

A second choice for Q_h: Let us assume that the number of edges of Σ_h is an even number. Then, we let Σ_{2h} be the partition of Γ_N arising by joining pairs of adjacent elements, and define for $k = 0$

$$Q_h \;:=\; \left\{ \boldsymbol{\lambda}_h \in \mathbf{H}_{00}^{1/2}(\Gamma_N) \;:\; \boldsymbol{\lambda}_h|_e \in \mathbf{P}_1(e) \quad \forall\, e \in \Sigma_{2h} \right\} . \tag{4.4}$$

As already stated in [9], the advantages and disadvantages of one choice or the other will become clear below from Lemma 4.1. More precisely, under quasi-uniformity assumptions on Σ_h and $\Sigma_{\tilde{h}}$, (4.3) allows any polynomial degree $k \geq 0$, whereas (4.4) is restricted to $k = 0$, but without requiring any condition on these meshes.

Then, the mixed finite element scheme associated with (3.9) reads: Find $((\mathbf{t}_h, \boldsymbol{\sigma}_h), \boldsymbol{\xi}_h) \in H_h \times Q_h$ such that

$$\begin{array}{rcll} [\mathcal{A}(\mathbf{t}_h, \boldsymbol{\sigma}_h), (\mathbf{s}_h, \boldsymbol{\tau}_h)] \;+\; [\mathcal{B}(\mathbf{s}_h, \boldsymbol{\tau}_h), \boldsymbol{\xi}_h] & = & [\mathcal{F}, (\mathbf{s}_h, \boldsymbol{\tau}_h)] & \forall\, (\mathbf{s}_h, \boldsymbol{\tau}_h) \in H_h, \\ [\mathcal{B}(\mathbf{t}_h, \boldsymbol{\sigma}_h), \boldsymbol{\lambda}_h] & = & [\mathcal{G}, \boldsymbol{\lambda}_h] & \forall\, \boldsymbol{\lambda}_h \in Q_h. \end{array} \tag{4.5}$$

We remark that the second identity in (2.4) suggests that the pressure p can be approximated later on by the postprocessing formula

$$p_h \;:=\; -\frac{1}{2}\, \mathrm{tr}\,(\boldsymbol{\sigma}_h) . \tag{4.6}$$

In what follows we apply again Theorem 3.1 to show that (4.5) is well-posed. We begin by recalling from [9] the discrete inf-sup condition for $\mathcal{B}$, which establishes the existence of $\beta > 0$, independent of h, such that

$$\sup_{\substack{(\mathbf{s}_h, \boldsymbol{\tau}_h) \in H_h \\ (\mathbf{s}_h, \boldsymbol{\tau}_h) \neq \mathbf{0}}} \frac{[\mathcal{B}(\mathbf{s}_h, \boldsymbol{\tau}_h), \boldsymbol{\lambda}_h]}{\|(\mathbf{s}_h, \boldsymbol{\tau}_h)\|_H} \;\geq\; \beta \|\boldsymbol{\lambda}_h\|_{0;1/2,\Gamma_N} \quad \forall\, \boldsymbol{\lambda}_h \in Q_h. \tag{4.7}$$

More precisely, we have the following result (cf. [9]).

Lemma 4.1. *Let Q_h be given by* (4.3) *and assume that both Σ_h and $\Sigma_{\tilde{h}}$ are quasi-uniform. Then there exist constants $C_0 \in (0, 1]$ and $\beta > 0$, independent of h and $\tilde{h}$, such that whenever $h_\Sigma \leq C_0 \tilde{h}$, there holds* (4.7). *Furthermore, let H_h and Q_h be given by* (4.1) *(with $k = 0$) and* (4.4), *respectively. Then there exists $\beta > 0$, independent of h, such that* (4.7) *holds.*

Proof. We first recall that the quasi-uniformity of Σ_h and, analogously, of $\Sigma_{\tilde{h}}$, means that there exists $c > 0$, independent of h, such that $\max\limits_{e \in \Sigma_h} |e| \leq c \min\limits_{e \in \Sigma_h} |e|$. We omit further details and refer to [9, Lemmas 5 and 6] for the proof of these results. □

On the other hand, the Lipschitz-continuity of $\mathcal{A}$ on $H_h \subseteq H$, follows similarly to the proof of Lemma 3.3. Hence, it remains to prove that for each $(\mathbf{r}_h, \boldsymbol{\rho}_h) \in H_h$, $\mathcal{A}((\mathbf{r}_h, \boldsymbol{\rho}_h) + \cdot\ )$ is uniformly strongly monotone on V_h, where V_h is the discrete kernel of the operator $\mathcal{B}$, that is

$$V_h \ := \ \mathbb{X}_h \times \widetilde{V}_h,$$

with

$$\widetilde{V}_h \ := \ \Big\{ \boldsymbol{\tau}_h \in \mathbb{RT}_k(\mathcal{T}_h) \ : \ \langle \boldsymbol{\tau}_h \boldsymbol{\nu}, \boldsymbol{\lambda}_h \rangle_{\Gamma_N} \ = \ 0 \quad \forall \ \boldsymbol{\lambda}_h \in Q_h \Big\}.$$

The following lemma provides the discrete analogue of Lemma 3.5.

Lemma 4.2. *There exists $C > 0$, independent of h, such that*

$$C \|\boldsymbol{\tau}_h\|^2_{\mathbf{div},\Omega} \ \leq \ \|\boldsymbol{\tau}_{0h}\|^2_{\mathbf{div},\Omega}, \quad \forall \ \boldsymbol{\tau}_h \ := \ \boldsymbol{\tau}_{0h} + d_h \mathbb{I} \in \widetilde{V}_h,$$

where $\boldsymbol{\tau}_{0h} \in \mathbb{RT}_k(\mathcal{T}_h) \cap \mathbb{H}_0(\mathbf{div}; \Omega)$ and $d_h \in R$.

Proof. See [9, Lemma 7]. □

Now, we are in a position to show the required discrete property of $\mathcal{A}$ on V_h, for all $(\mathbf{r}_h, \boldsymbol{\rho}_h) \in H_h$.

Lemma 4.3. *Assume that the parameter κ lies in $\left(0, \frac{2\alpha_0 \delta}{\gamma_0}\right)$ for each $\delta \in \left(0, \frac{2}{\gamma_0}\right)$, where α_0 and γ_0 are the positive constants from (2.2) and (2.3). Then, there exists a constant $C > 0$, independent of h, such that*

$$[\mathcal{A}((\mathbf{r}_h, \boldsymbol{\rho}_h) + (\mathbf{t}_h, \boldsymbol{\sigma}_h)) - \mathcal{A}((\mathbf{r}_h, \boldsymbol{\rho}_h) + (\mathbf{s}_h, \boldsymbol{\tau}_h)), (\mathbf{t}_h, \boldsymbol{\sigma}_h) - (\mathbf{s}_h, \boldsymbol{\tau}_h)] \ \geq \ C \|(\mathbf{t}_h, \boldsymbol{\sigma}_h) - (\mathbf{s}_h, \boldsymbol{\tau}_h)\|^2_H \,,$$

for all $(\mathbf{r}_h, \boldsymbol{\rho}_h) \in H_h$, and for all $(\mathbf{t}_h, \boldsymbol{\sigma}_h), (\mathbf{s}_h, \boldsymbol{\tau}_h) \in V_h$.

Proof. It follows straightforwardly from the proof of Lemma 3.6, using now Lemma 4.2 instead of Lemma 3.5. □

The following theorem establishes the well posedness of (4.5) and the associated Céa estimate.

Theorem 4.1. *Let Q_h be any of the two choices described above with the conditions assumed in* Lemma 4.1. *Also, suppose that the parameter κ lies in $\left(0, \frac{2\alpha_0 \delta}{\gamma_0}\right)$ for each $\delta \in \left(0, \frac{2}{\gamma_0}\right)$, where α_0 and γ_0 are the positive constants from (2.2) and (2.3). Then the Galerkin scheme (4.5) has a unique solution $((\mathbf{t}_h, \boldsymbol{\sigma}_h), \boldsymbol{\xi}_h) \in H_h \times Q_h$ and there exist positive constants $C_1, C_2 > 0$, independent of h, such that*

$$\|((\mathbf{t}_h, \boldsymbol{\sigma}_h), \boldsymbol{\xi}_h)\|_{H \times Q} \ \leq \ C_1 \Big\{ \|\mathbf{f}\|_{0,\Omega} \ + \ \|\mathbf{g}\|_{-1/2,\Gamma_N} \Big\}, \tag{4.8}$$

and

$$\begin{aligned} &\|((\mathbf{t}, \boldsymbol{\sigma}), \boldsymbol{\xi}) - ((\mathbf{t}_h, \boldsymbol{\sigma}_h), \boldsymbol{\xi}_h)\|_{H \times Q} \\ &\leq \ C_2 \left\{ \inf_{(\mathbf{s}_h, \boldsymbol{\tau}_h) \in H_h} \|(\mathbf{t}, \boldsymbol{\sigma}) - (\mathbf{s}_h, \boldsymbol{\tau}_h)\|_H \ + \ \inf_{\boldsymbol{\lambda}_h \in Q_h} \|\boldsymbol{\xi} - \boldsymbol{\lambda}_h\|_{0;1/2,\Gamma_N} \right\}. \end{aligned} \tag{4.9}$$

Proof. Thanks to the previous results given by Lemmas 4.1, 3.3 and 4.3, the proof is again a direct application of Theorem 3.1. In turn, the Céa estimate (4.9) follows from a particular application of the general result given by [23, Theorem 2.1]. □

Next, in order to provide the rate of convergence of the Galerkin scheme (4.5), we need the approximation properties of the finite element subspaces involved. For this purpose, we now introduce the Raviart-Thomas interpolation operator (see [2, 21]) $\Pi_h^k : \mathbb{H}^1(\Omega) \to \mathbb{RT}_k(\mathcal{T}_h)$, which, given $\boldsymbol{\tau} \in \mathbb{H}^1(\Omega)$, is characterized by the following identities:

$$\int_e \Pi_h^k(\boldsymbol{\tau})\boldsymbol{\nu} \cdot \mathbf{p} \;=\; \int_e \boldsymbol{\tau}\boldsymbol{\nu} \cdot \mathbf{p}, \quad \forall \text{ edge } e \in \mathcal{T}_h, \quad \forall\, \mathbf{p} \in \mathbf{P}_k(e), \quad \text{when } k \geq 0, \tag{4.10}$$

and

$$\int_T \Pi_h^k(\boldsymbol{\tau}) : \boldsymbol{\rho} \;=\; \int_T \boldsymbol{\tau} : \boldsymbol{\rho}, \quad \forall\, T \in \mathcal{T}_h, \quad \forall\, \boldsymbol{\rho} \in \mathbb{P}_{k-1}(T), \quad \text{when } k \geq 1. \tag{4.11}$$

Recall, according to the notations introduced in Section 1, that $\mathbf{P}_k(e) := [P_k(e)]^2$ and $\mathbb{P}_{k-1}(T) := [P_{k-1}(T)]^{2\times 2}$. Then, it is easy to show, using (4.10) and (4.11), that (cf. [20, Section 3.4.2, eq. (3.4.23)])

$$\mathbf{div}(\Pi_h^k(\boldsymbol{\tau})) \;=\; \mathcal{P}_h^k(\mathbf{div}(\boldsymbol{\tau})), \tag{4.12}$$

where $\mathcal{P}_h^k : \mathbf{L}^2(\Omega) \to \mathcal{Q}_h^{\mathbf{u}}$ is the $\mathbf{L}^2(\Omega)$-orthogonal projector. Since $\mathcal{Q}_h^{\mathbf{u}}$ is the subspace of $\mathbf{L}^2(\Omega)$ formed by piecewise polynomial vectors of degree $\leq k$ [cf. (4.2)], it is easy to see that $\mathcal{P}_h^k(\mathbf{v})|_T = \mathcal{P}_{h,T}^k(\mathbf{v}|_T)$ for each $T \in \mathcal{T}_h$, for each $\mathbf{v} \in \mathbf{L}^2(\Omega)$, where $\mathcal{P}_{h,T}^k : \mathbf{L}^2(T) \to \mathbf{P}_k(T)$ is the local orthogonal projector. Hence, for each $\mathbf{v} \in \mathbf{H}^m(\Omega)$, with $0 \leq m \leq k+1$, there holds (see, e.g. [4])

$$\|\mathbf{v} - \mathcal{P}_h^k(\mathbf{v})\|_{0,T} \;=\; \|\mathbf{v} - \mathcal{P}_{h,T}^k(\mathbf{v})\|_{0,T} \;\leq\; Ch_T^m |\mathbf{v}|_{m,T} \quad \forall\, T \in \mathcal{T}_h. \tag{4.13}$$

In addition, the operator Π_h^k satisfies the following approximation properties (see, e.g. [2, 21]): for each $\boldsymbol{\tau} \in \mathbb{H}^m(\Omega)$, with $1 \leq m \leq k+1$, there holds

$$\|\boldsymbol{\tau} - \Pi_h^k(\boldsymbol{\tau})\|_{0,T} \;\leq\; Ch_T^m |\boldsymbol{\tau}|_{m,T} \quad \forall\, T \in \mathcal{T}_h, \tag{4.14}$$

for each $\boldsymbol{\tau} \in \mathbb{H}^1(\Omega)$ such that $\mathbf{div}(\boldsymbol{\tau}) \in \mathbf{H}^m(\Omega)$, with $0 \leq m \leq k+1$, there holds

$$\|\mathbf{div}(\boldsymbol{\tau} - \Pi_h^k(\boldsymbol{\tau}))\|_{0,T} \;\leq\; Ch_T^m |\mathbf{div}(\boldsymbol{\tau})|_{m,T} \quad \forall\, T \in \mathcal{T}_h, \tag{4.15}$$

and for each $\boldsymbol{\tau} \in \mathbb{H}^1(\Omega)$, there holds

$$\|\boldsymbol{\tau}\boldsymbol{\nu} - \Pi_h^k(\boldsymbol{\tau})\boldsymbol{\nu}\|_{0,e} \;\leq\; Ch_e^{1/2} \|\boldsymbol{\tau}\|_{1,T_e} \quad \forall \text{ edge } e \in \mathcal{T}_h, \tag{4.16}$$

where $T_e \in \mathcal{T}_h$ contains e on its boundary. In particular, note that (4.15) follows easily from (4.12) and (4.13). Moreover, the interpolation operator Π_h^k can also be defined as a bounded linear operator from the larger space $\mathbb{H}^s(\Omega) \cap \mathbb{H}(\mathbf{div};\Omega)$ into $\mathbb{RT}_k(\mathcal{T}_h)$ for all $s \in (0,1]$ (see, e.g. [15, Theorem 3.16]), and in this case there holds the following interpolation error estimate

$$\|\boldsymbol{\tau} - \Pi_h^k(\boldsymbol{\tau})\|_{0,T} \;\leq\; Ch_T^s \Big\{ \|\boldsymbol{\tau}\|_{s,T} \;+\; \|\mathbf{div}(\boldsymbol{\tau})\|_{0,T} \Big\} \quad \forall\, T \in \mathcal{T}_h. \tag{4.17}$$

Then, as a consequence of (4.13)–(4.17) and the usual estimates for the interpolation in Sobolev spaces (cf. [19, Appendix B]), we find that $\mathbb{X}_h$, $\mathbb{RT}_k(\mathcal{T}_h)$ and Q_h satisfy the following approximation properties:

($\mathbf{AP}_h^{\mathbf{t}}$) For each $s \in [0, k+1]$ and for each $\mathbf{s} \in \mathbb{H}^s(\Omega)$ there exists $\mathbf{s}_h \in \mathbb{X}_h$ such that

$$\|\mathbf{s} - \mathbf{s}_h\|_{0,\Omega} \;\leq\; Ch^s \|\mathbf{s}\|_{s,\Omega}.$$

($\mathbf{AP}_h^{\boldsymbol{\sigma}}$) For each $s \in (0, k+1]$ and for each $\boldsymbol{\tau} \in \mathbb{H}^s(\Omega)$ with $\mathbf{div}(\boldsymbol{\tau}) \in \mathbf{H}^s(\Omega)$ there exists $\boldsymbol{\tau}_h \in \mathbb{RT}_k(\mathcal{T}_h)$ such that

$$\|\boldsymbol{\tau} - \boldsymbol{\tau}_h\|_{\mathbf{div},\Omega} \ \leq \ Ch^s \Big\{ \|\boldsymbol{\tau}\|_{s,\Omega} \ + \ \|\mathbf{div}(\boldsymbol{\tau})\|_{s,\Omega} \Big\}.$$

($\mathbf{AP}_h^{\boldsymbol{\xi}}$) For each $s \in [0, k+1]$ and for each $\boldsymbol{\lambda} \in \mathbf{H}_{00}^{s+1/2}(\Gamma_N)$, there exists $\boldsymbol{\lambda}_h \in Q_h$ such that

$$\|\boldsymbol{\lambda} - \boldsymbol{\lambda}_h\|_{0;1/2,\Gamma_N} \ \leq \ Ch^s \|\boldsymbol{\lambda}\|_{s+1/2,\Gamma_N}.$$

The following theorem provides the theoretical rate of convergence of the Galerkin scheme (4.5), under suitable regularity assumptions on the exact solution.

Theorem 4.2. *Let $((\mathbf{t}, \boldsymbol{\sigma}), \boldsymbol{\xi}) \in H \times Q$ and $((\mathbf{t}_h, \boldsymbol{\sigma}_h), \boldsymbol{\xi}_h) \in H_h \times Q_h$ be the unique solutions of the continuous and discrete formulations* (3.9) *and* (4.5)*, respectively. Assume that $\mathbf{t} \in \mathbb{H}^s(\Omega)$, $\boldsymbol{\sigma} \in \mathbb{H}^s(\Omega)$, $\mathbf{div}(\boldsymbol{\sigma}) \in \mathbf{H}^s(\Omega)$ and $\boldsymbol{\xi} \in \mathbf{H}_{00}^{s+1/2}(\Gamma_N)$, for some $s \in (0, k+1]$. Then, there exists $C > 0$, independent of h, such that*

$$\|((\mathbf{t}, \boldsymbol{\sigma}), \boldsymbol{\xi}) - ((\mathbf{t}_h, \boldsymbol{\sigma}_h), \boldsymbol{\xi}_h)\|_{H \times Q} \ \leq \ Ch^s \left\{ \|\mathbf{t}\|_{s,\Omega} + \|\boldsymbol{\sigma}\|_{s,\Omega} + \|\mathbf{div}(\boldsymbol{\sigma})\|_{s,\Omega} + \|\boldsymbol{\xi}\|_{s+1/2,\Gamma_N} \right\}.$$

Proof. It follows from the Céa estimate (4.9) (cf. Theorem 4.1) and the approximation properties ($\mathbf{AP}_h^{\mathbf{t}}$), ($\mathbf{AP}_h^{\boldsymbol{\sigma}}$) and ($\mathbf{AP}_h^{\boldsymbol{\xi}}$). □

5 A residual-based a posteriori error estimator

In this section we develop a residual-based a-posteriori error analysis for the mixed finite element scheme (4.5).

5.1 Preliminaries

First we introduce several notations. Given $T \in \mathcal{T}_h$, we let $\mathcal{E}(T)$ be the set of its edges, and let $\mathcal{E}_h$ be the set of all edges of the triangulation $\mathcal{T}_h$. Then we write $\mathcal{E}_h = \mathcal{E}_h(\Omega) \cup \mathcal{E}_h(\Gamma_D) \cup \mathcal{E}_h(\Gamma_N)$, where $\mathcal{E}_h(\Omega) := \{e \in \mathcal{E}_h : e \subseteq \Omega\}$, $\mathcal{E}_h(\Gamma_D) := \{e \in \mathcal{E}_h : e \subseteq \Gamma_D\}$ and $\mathcal{E}_h(\Gamma_N) := \{e \in \mathcal{E}_h : e \subseteq \Gamma_N\}$. Also, for each edge $e \in \mathcal{E}_h$ we fix a unit normal vector $\boldsymbol{\nu}_e := (\nu_1, \nu_2)^{\mathrm{t}}$, and let $\boldsymbol{s}_e := (-\nu_2, \nu_1)^{\mathrm{t}}$ be the corresponding fixed unit tangential vector along e. Then, given $e \in \mathcal{E}_h(\Omega)$ and $\boldsymbol{\tau} \in \mathbb{L}^2(\Omega)$ such that $\boldsymbol{\tau}|_T \in \mathbb{C}(T) := [C(T)]^{2\times 2}$ on each $T \in \mathcal{T}_h$, we let $[\![\boldsymbol{\tau}\boldsymbol{s}_e]\!]$ be the corresponding jump across e, that is, $[\![\boldsymbol{\tau}\boldsymbol{s}_e]\!] := (\boldsymbol{\tau}|_T - \boldsymbol{\tau}|_{T'})|_e \boldsymbol{s}_e$, where T and T' are the triangles of $\mathcal{T}_h$ having e as a common edge. Abusing notation, when $e \in \mathcal{E}_h(\Gamma)$, we also write $[\![\boldsymbol{\tau}\boldsymbol{s}_e]\!] := \boldsymbol{\tau}|_e \boldsymbol{s}_e$. From now on, when no confusion arises, we simple write $\boldsymbol{s}$ and $\boldsymbol{\nu}$ instead of $\boldsymbol{s}_e$ and $\boldsymbol{\nu}_e$, respectively. Finally, given scalar, vector and tensor valued fields v, $\boldsymbol{\varphi} := (\varphi_1, \varphi_2)$ and $\boldsymbol{\tau} := (\tau_{ij})$, respectively, we let

$$\mathbf{curl}(v) \ := \ \begin{pmatrix} \frac{\partial v}{\partial x_2} \\ -\frac{\partial v}{\partial x_1} \end{pmatrix}, \quad \underline{\mathbf{curl}}(\boldsymbol{\varphi}) \ := \ \begin{pmatrix} \mathbf{curl}(\varphi_1)^{\mathrm{t}} \\ \mathbf{curl}(\varphi_2)^{\mathrm{t}} \end{pmatrix}, \quad \text{and} \quad \mathrm{curl}(\boldsymbol{\tau}) \ := \ \begin{pmatrix} \frac{\partial \tau_{12}}{\partial x_1} - \frac{\partial \tau_{11}}{\partial x_2} \\ \frac{\partial \tau_{22}}{\partial x_1} - \frac{\partial \tau_{21}}{\partial x_2} \end{pmatrix}.$$

Then, letting $((\mathbf{t}, \boldsymbol{\sigma}), \boldsymbol{\xi}) \in H \times Q$ and $((\mathbf{t}_h, \boldsymbol{\sigma}_h), \boldsymbol{\xi}_h) \in H_h \times Q_h$ be the unique solutions of the continuous and discrete formulations (3.9) and (4.5), respectively, we define for each $T \in \mathcal{T}_h$ a local error indicator

θ_T as follows:

$$\begin{aligned}\theta_T^2 \;:=\; & \frac{1}{\alpha^2}\|\mathbf{f}-\mathcal{P}_h^k(\mathbf{f})\|_{0,T}^2+h_T^2\,\|\mathbf{t}_h-\nabla\mathbf{u}_h\|_{0,T}^2+h_T^2\|\mathrm{curl}(\mathbf{t}_h)\|_{0,T}^2\\ & +\sum_{e\in\mathcal{E}(T)\cap\mathcal{E}_h(\Omega)}h_e\|[\![\mathbf{t}_h\boldsymbol{s}]\!]\|_{0,e}^2+\sum_{e\in\mathcal{E}(T)\cap\mathcal{E}_h(\Gamma_D)}h_e\|[\![\mathbf{t}_h\boldsymbol{s}]\!]\|_{0,e}^2\\ & +\sum_{e\in\mathcal{E}(T)\cap\mathcal{E}_h(\Gamma_N)}h_e\left\{\left\|\mathbf{t}_h\boldsymbol{s}+\frac{d\boldsymbol{\xi}_h}{d\boldsymbol{s}}\right\|_{0,e}^2+\|\boldsymbol{\xi}_h+\mathbf{u}_h\|_{0,e}^2+\|\mathbf{g}-\boldsymbol{\sigma}_h\boldsymbol{\nu}\|_{0,e}^2\right\}\\ & +\|\boldsymbol{\sigma}_h^{\mathrm{d}}-\boldsymbol{\psi}(\mathbf{t}_h)\|_{0,T}^2+h_T^2\|\mathrm{curl}\left(\boldsymbol{\sigma}_h^{\mathrm{d}}-\boldsymbol{\psi}(\mathbf{t}_h)\right)\|_{0,T}^2\\ & +\sum_{e\in\mathcal{E}(T)}h_e\|[\![(\boldsymbol{\sigma}_h^{\mathrm{d}}-\boldsymbol{\psi}(\mathbf{t}_h))\boldsymbol{s}]\!]\|_{0,e}^2, \end{aligned}\tag{5.1}$$

where, resembling (3.7), we set

$$\mathbf{u}_h \;:=\; \frac{1}{\alpha}\left\{\mathcal{P}_h^k(\mathbf{f})\;+\;\mathbf{div}(\boldsymbol{\sigma}_h)\right\}\quad\text{in }\Omega.\tag{5.2}$$

Note that the term $\|\mathbf{g}-\boldsymbol{\sigma}_h\boldsymbol{\nu}\|_{0,e}^2$, defining θ_T^2, requires that $\mathbf{g}|_e\in\mathbf{L}^2(e)\;\forall\;e\in\mathcal{E}_h(\Gamma_N)$. The residual character of each term on the right hand side of (5.1) is quite clear. As usual the expression

$$\boldsymbol{\theta}\;:=\;\left\{\sum_{T\in\mathcal{T}_h}\theta_T^2\right\}^{1/2}\tag{5.3}$$

is employed as the global residual error estimator.

The following theorem constitutes the main result of this section.

Theorem 5.1. *Let $((\mathbf{t},\boldsymbol{\sigma}),\boldsymbol{\xi})\in H\times Q$ and $((\mathbf{t}_h,\boldsymbol{\sigma}_h),\boldsymbol{\xi}_h)\in H_h\times Q_h$ be the unique solutions of* (3.9) *and* (4.5)*, respectively. In addition, let $\mathbf{u}\in\mathbf{L}^2(\Omega)$ be defined according to* (3.7)*, that is $\mathbf{u}:=\frac{1}{\alpha}\{\mathbf{f}+\mathbf{div}(\boldsymbol{\sigma})\}$, and assume that the Neumann datum $\mathbf{g}$ belongs to $\mathbf{L}^2(\Gamma_N)$. Then, there exists positive constants $C_{\mathtt{eff}}$ and $C_{\mathtt{rel}}$, independent of h, such that*

$$C_{\mathtt{eff}}\boldsymbol{\theta}+h.o.t.\;\le\;\|\mathbf{u}-\mathbf{u}_h\|_{0,\Omega}\;+\;\|((\mathbf{t}-\mathbf{t}_h,\boldsymbol{\sigma}-\boldsymbol{\sigma}_h),\boldsymbol{\xi}-\boldsymbol{\xi}_h)\|_{H\times Q}\;\le\;C_{\mathtt{rel}}\boldsymbol{\theta},\tag{5.4}$$

where h.o.t. stands for one or several terms of higher order.

The proof of Theorem 5.1, which follows closely the approaches in [6] and [9], is separated into the two parts given by the next subsections. The efficiency of the global error estimator (lower bound in (5.4)) is proved below in Section 5.3, whereas the corresponding reliability (upper bound in (5.4)) is derived next. The meaning of *h.o.t.* is explained below right after Lemma 5.12.

5.2 Reliability

We begin by recalling from the proof of Lemma 3.2 that $\mathcal{D}\mathbb{A}(\widetilde{\mathbf{r}})$ is a uniformly bounded and uniformly elliptic bilinear form on $\mathbb{L}^2_{\mathrm{tr}}(\Omega)\times\mathbb{L}^2_{\mathrm{tr}}(\Omega)$ for all $\widetilde{\mathbf{r}}\in\mathbb{L}^2_{\mathrm{tr}}(\Omega)$. Moreover, we observe from (3.10) and (3.15), that the nonlinear operator $\mathcal{A}$ can be rewritten as:

$$[\mathcal{A}(\mathbf{t},\boldsymbol{\sigma}),(\mathbf{s},\boldsymbol{\tau})]\;:=\;[\mathbb{A}(\mathbf{t}),\mathbf{s}-\kappa\boldsymbol{\tau}^{\mathrm{d}}]-\int_\Omega\mathbf{s}:\boldsymbol{\sigma}^{\mathrm{d}}+\int_\Omega\mathbf{t}:\boldsymbol{\tau}^{\mathrm{d}}+\kappa\int_\Omega\boldsymbol{\sigma}^{\mathrm{d}}:\boldsymbol{\tau}^{\mathrm{d}}+\frac{1}{\alpha}\int_\Omega\mathbf{div}(\boldsymbol{\sigma})\cdot\mathbf{div}(\boldsymbol{\tau})\,.\tag{5.5}$$

Hence, as a consequence of the continuous dependence result provided by the linear version of Theorem 3.1 (cf. (3.13) and (3.14) with $\mathcal{A}$ linear), which is actually the usual estimate provided by the Babuška-Brezzi theory (see, e.g. [2, Theorem 1.1 in Chapter II]), we can conclude that the linear operator $\mathcal{M}$ obtained by adding the two equations of the left hand side of (3.9), after replacing $\mathbb{A}$ within $\mathcal{A}$ (see (5.5)) by the Gâteaux derivative $\mathcal{D}\mathbb{A}(\widetilde{\mathbf{r}})$ at any $\widetilde{\mathbf{r}} \in \mathbb{L}^2_{\mathrm{tr}}(\Omega)$, satisfies a global inf-sup condition. More precisely, there exists a constant $C > 0$ such that

$$C\|((\mathbf{r},\boldsymbol{\rho}),\boldsymbol{\zeta})\|_{H\times Q} \;\leq\; \sup_{\substack{((\mathbf{s},\boldsymbol{\tau}),\boldsymbol{\lambda})\in H\times Q\\ ((\mathbf{s},\boldsymbol{\tau}),\boldsymbol{\lambda})\neq \mathbf{0}}} \frac{[\mathcal{M}((\mathbf{s},\boldsymbol{\tau}),\boldsymbol{\lambda}),((\mathbf{r},\boldsymbol{\rho}),\boldsymbol{\zeta})]}{\|((\mathbf{s},\boldsymbol{\tau}),\boldsymbol{\lambda})\|_{H\times Q}}, \tag{5.6}$$

for all $\widetilde{\mathbf{r}} \in \mathbb{L}^2_{\mathrm{tr}}(\Omega)$ and for all $((\mathbf{r},\boldsymbol{\rho}),\boldsymbol{\zeta}) \in H \times Q$, where

$$\begin{aligned}[\mathcal{M}((\mathbf{s},\boldsymbol{\tau}),\boldsymbol{\lambda}),((\mathbf{r},\boldsymbol{\rho}),\boldsymbol{\zeta})] \;&:=\; \mathcal{D}\mathbb{A}(\widetilde{\mathbf{r}})(\mathbf{r},\mathbf{s}-\kappa\boldsymbol{\tau}^{\mathrm{d}}) - \int_\Omega \mathbf{s}:\boldsymbol{\rho}^{\mathrm{d}} + \int_\Omega \mathbf{r}:\boldsymbol{\tau}^{\mathrm{d}}\\ &+\quad \kappa\int_\Omega \boldsymbol{\rho}^{\mathrm{d}}:\boldsymbol{\tau}^{\mathrm{d}} + \frac{1}{\alpha}\int_\Omega \mathbf{div}(\boldsymbol{\rho})\cdot\mathbf{div}(\boldsymbol{\tau}) \;+\; [\mathcal{B}(\mathbf{s},\boldsymbol{\tau}),\boldsymbol{\zeta}] \;+\; [\mathcal{B}(\mathbf{r},\boldsymbol{\rho}),\boldsymbol{\lambda}]\,.\end{aligned}$$

We now have the following preliminary estimate.

Lemma 5.1. *Let $((\mathbf{t},\boldsymbol{\sigma}),\boldsymbol{\xi}) \in H\times Q$ and $((\mathbf{t}_h,\boldsymbol{\sigma}_h),\boldsymbol{\xi}_h) \in H_h\times Q_h$ be the unique solutions of* (3.9) *and* (4.5)*, respectively. Then there exists $C>0$, independent of h, such that*

$$\begin{aligned}&C\,\|((\mathbf{t}-\mathbf{t}_h,\boldsymbol{\sigma}-\boldsymbol{\sigma}_h),\boldsymbol{\xi}-\boldsymbol{\xi}_h)\|_{H\times Q}\\ &\qquad\leq\; \|\boldsymbol{\sigma}_h^{\mathrm{d}}-\boldsymbol{\psi}(\mathbf{t}_h)\|_{0,\Omega} \;+\; \|\mathbf{g}-\boldsymbol{\sigma}_h\boldsymbol{\nu}\|_{-1/2,\Gamma_N} \;+\; \sup_{\substack{\boldsymbol{\tau}\in\mathbb{H}(\mathbf{div};\Omega)\\ \boldsymbol{\tau}\neq\mathbf{0}}} \frac{\big(E_1+E_2\big)(\boldsymbol{\tau})}{\|\boldsymbol{\tau}\|_{\mathbf{div},\Omega}}\,,\end{aligned} \tag{5.7}$$

where the functionals E_1 and E_2, defined as

$$E_1(\boldsymbol{\tau}) \;:=\; \langle\boldsymbol{\tau}\boldsymbol{\nu},\boldsymbol{\xi}_h\rangle_{\Gamma_N} + \int_\Omega \mathbf{t}_h:\boldsymbol{\tau} + \frac{1}{\alpha}\int_\Omega (\mathbf{f}+\mathbf{div}(\boldsymbol{\sigma}_h))\cdot\mathbf{div}(\boldsymbol{\tau})\,, \tag{5.8}$$

and

$$E_2(\boldsymbol{\tau}) \;:=\; \kappa\int_\Omega (\boldsymbol{\sigma}_h^{\mathrm{d}}-\boldsymbol{\psi}(\mathbf{t}_h)):\boldsymbol{\tau}\,, \tag{5.9}$$

satisfy

$$\big(E_1+E_2\big)(\boldsymbol{\tau}_h) \;=\; 0 \qquad \forall\,\boldsymbol{\tau}_h \in \mathbb{RT}_k(\mathcal{T}_h)\,. \tag{5.10}$$

Proof. Since $\mathbf{t}$ and $\mathbf{t}_h$ belong to $\mathbb{L}^2_{\mathrm{tr}}(\Omega)$, a straightforward application of the mean value theorem yields the existence of a convex combination of $\mathbf{t}$ and $\mathbf{t}_h$, say $\widetilde{\mathbf{r}}_h \in \mathbb{L}^2_{\mathrm{tr}}(\Omega)$, such that

$$\mathcal{D}\mathbb{A}(\widetilde{\mathbf{r}}_h)(\mathbf{t}-\mathbf{t}_h,\mathbf{s}) \;=\; [\mathbb{A}(\mathbf{t})-\mathbb{A}(\mathbf{t}_h),\mathbf{s}] \quad \forall\,\mathbf{s}\in\mathbb{L}^2_{\mathrm{tr}}(\Omega).$$

Then, applying (5.6) to the Galerkin error $((\mathbf{r},\boldsymbol{\rho}),\boldsymbol{\zeta}) := ((\mathbf{t}-\mathbf{t}_h,\boldsymbol{\sigma}-\boldsymbol{\sigma}_h),\boldsymbol{\xi}-\boldsymbol{\xi}_h)$, we obtain that

$$\begin{aligned}&C\|((\mathbf{t}-\mathbf{t}_h,\boldsymbol{\sigma}-\boldsymbol{\sigma}_h),\boldsymbol{\xi}-\boldsymbol{\xi}_h)\|_{H\times Q}\\ &\leq \sup_{\substack{((\mathbf{s},\boldsymbol{\tau}),\boldsymbol{\lambda})\in H\times Q\\ ((\mathbf{s},\boldsymbol{\tau}),\boldsymbol{\lambda})\neq\mathbf{0}}} \frac{[\mathcal{A}(\mathbf{t},\boldsymbol{\sigma})-\mathcal{A}(\mathbf{t}_h,\boldsymbol{\sigma}_h),(\mathbf{s},\boldsymbol{\tau})] + [\mathcal{B}(\mathbf{s},\boldsymbol{\tau}),\boldsymbol{\xi}-\boldsymbol{\xi}_h] + [\mathcal{B}(\mathbf{t}-\mathbf{t}_h,\boldsymbol{\sigma}-\boldsymbol{\sigma}_h),\boldsymbol{\lambda}]}{\|((\mathbf{s},\boldsymbol{\tau}),\boldsymbol{\lambda})\|_{H\times Q}}\\ &\leq \sup_{\substack{(\mathbf{s},\boldsymbol{\tau})\in H\\ (\mathbf{s},\boldsymbol{\tau})\neq\mathbf{0}}} \frac{\mathcal{R}(\mathbf{s},\boldsymbol{\tau})}{\|(\mathbf{s},\boldsymbol{\tau})\|_H} \;+\; \sup_{\substack{\boldsymbol{\lambda}\in Q\\ \boldsymbol{\lambda}\neq\mathbf{0}}} \frac{[\mathcal{B}(\mathbf{t}-\mathbf{t}_h,\boldsymbol{\sigma}-\boldsymbol{\sigma}_h),\boldsymbol{\lambda}]}{\|\boldsymbol{\lambda}\|_{0;1/2,\Gamma_N}},\end{aligned} \tag{5.11}$$

where $\mathcal{R}(\mathbf{s},\boldsymbol{\tau}) := [\mathcal{A}(\mathbf{t},\boldsymbol{\sigma}) - \mathcal{A}(\mathbf{t}_h,\boldsymbol{\sigma}_h),(\mathbf{s},\boldsymbol{\tau})] + [\mathcal{B}(\mathbf{s},\boldsymbol{\tau}),\boldsymbol{\xi}-\boldsymbol{\xi}_h]$. But, from the second equation of (3.9) and the definitions of $\mathcal{B}$ (cf. (3.11)) and $\mathcal{G}$ (cf. (3.12)), we see that $[\mathcal{B}(\mathbf{t}-\mathbf{t}_h,\boldsymbol{\sigma}-\boldsymbol{\sigma}_h),\boldsymbol{\lambda}] = \langle \mathbf{g}-\boldsymbol{\sigma}_h\boldsymbol{\nu},\boldsymbol{\lambda}\rangle_{\Gamma_N}$, which yields

$$\sup_{\substack{\boldsymbol{\lambda}\in Q\\ \boldsymbol{\lambda}\neq\mathbf{0}}} \frac{[\mathcal{B}(\mathbf{t}-\mathbf{t}_h,\boldsymbol{\sigma}-\boldsymbol{\sigma}_h),\boldsymbol{\lambda}]}{\|\boldsymbol{\lambda}\|_{0;1/2,\Gamma_N}} \;=\; \sup_{\substack{\boldsymbol{\lambda}\in Q\\ \boldsymbol{\lambda}\neq\mathbf{0}}} \frac{\langle \mathbf{g}-\boldsymbol{\sigma}_h\boldsymbol{\nu},\boldsymbol{\lambda}\rangle_{\Gamma_N}}{\|\boldsymbol{\lambda}\|_{0;1/2,\Gamma_N}} \;=\; \|\mathbf{g}-\boldsymbol{\sigma}_h\boldsymbol{\nu}\|_{-1/2,\Gamma_N}\,. \tag{5.12}$$

Next, according to the first equation of (3.9) we observe that

$$\mathcal{R}(\mathbf{s},\boldsymbol{\tau}) \;=\; [\mathcal{F},(\mathbf{s},\boldsymbol{\tau})] - [\mathcal{A}(\mathbf{t}_h,\boldsymbol{\sigma}_h),(\mathbf{s},\boldsymbol{\tau})] - [\mathcal{B}(\mathbf{s},\boldsymbol{\tau}),\boldsymbol{\xi}_h] \quad \forall\,(\mathbf{s},\boldsymbol{\tau})\in H\,,$$

which gives

$$\mathcal{R}(\mathbf{s},\boldsymbol{\tau}) \;=\; -E_1(\boldsymbol{\tau}) - E_2(\boldsymbol{\tau}) + \int_\Omega (\boldsymbol{\sigma}_h^{\mathrm{d}} - \boldsymbol{\psi}(\mathbf{t}_h)) : \mathbf{s} \quad \forall\,(\mathbf{s},\boldsymbol{\tau})\in H\,. \tag{5.13}$$

Then, applying the Cauchy-Schwarz inequality to the last term on the right hand side of (5.13), and replacing the resulting expression together with (5.12) back into (5.11), we obtain (5.7). Finally, it is easy to see from (5.13) and the first equation of (4.5) that (5.10) holds. □

We now aim to bound the supremum on the right hand side of (5.7), for which we write

$$\big(E_1+E_2\big)(\boldsymbol{\tau}) \;=\; E_1(\boldsymbol{\tau}-\boldsymbol{\tau}_h) \;+\; E_2(\boldsymbol{\tau}-\boldsymbol{\tau}_h) \tag{5.14}$$

with a suitable choice of $\boldsymbol{\tau}_h \in \mathbb{RT}_k(\mathcal{T}_h)$. To this end, and proceeding exactly as in [9, Section 4.2], we need the Clément interpolation operator $\mathcal{I}_h : H^1(\Omega) \to X_h$ (cf. [5]), where

$$X_h \;:=\; \big\{ v\in C(\bar\Omega) \;:\; v|_T \in P_1(T) \quad \forall\, T\in\mathcal{T}_h \big\}\,.$$

A vectorial version of $\mathcal{I}_h$, say $\boldsymbol{\mathcal{I}}_h : \mathbf{H}^1(\Omega) \to \mathbf{X}_h$, which is defined componentwise by $\mathcal{I}_h$, is also required. The following lemma establishes the local approximation properties of $\mathcal{I}_h$.

Lemma 5.2. *There exist constants $c_1, c_2 > 0$, independent of h, such that for all $v\in H^1(\Omega)$ there holds*

$$\|v-\mathcal{I}_h(v)\|_{0,T} \;\leq\; c_1 h_T \|v\|_{1,\Delta(T)} \quad \forall\, T\in\mathcal{T}_h,$$

and

$$\|v-\mathcal{I}_h(v)\|_{0,e} \;\leq\; c_2 h_e^{1/2} \|v\|_{1,\Delta(e)} \quad \forall\, e\in\mathcal{E}_h,$$

where $\Delta(T)$ and $\Delta(e)$ are the union of all elements intersecting with T and e, respectively.

Proof. See [5]. □

Next, for each $\boldsymbol{\tau}\in\mathbb{H}(\mathbf{div};\Omega)$ we consider its Helmholtz decomposition (see, e.g. [9, Section 4.2] for details)

$$\boldsymbol{\tau} \;=\; \nabla\mathbf{z} + \underline{\mathbf{curl}}(\boldsymbol{\chi})\,, \tag{5.15}$$

where $\mathbf{z}\in\mathbf{H}^2(\Omega)$ and $\boldsymbol{\chi}\in\mathbf{H}^1(\Omega)$ satisfy $\Delta\mathbf{z} = \mathbf{div}(\boldsymbol{\tau})$ in Ω, $\int_\Omega \boldsymbol{\chi} = \mathbf{0}$, and

$$\|\mathbf{z}\|_{2,\Omega} + \|\boldsymbol{\chi}\|_{1,\Omega} \;\leq\; C\|\boldsymbol{\tau}\|_{\mathbf{div},\Omega}\,. \tag{5.16}$$

Then, we let $\boldsymbol{\zeta} := \nabla\mathbf{z}\in\mathbb{H}^1(\Omega)$, $\boldsymbol{\chi}_h := \boldsymbol{\mathcal{I}}_h(\boldsymbol{\chi})$, and define

$$\boldsymbol{\tau}_h \;:=\; \Pi_h^k(\boldsymbol{\zeta}) \;+\; \underline{\mathbf{curl}}(\boldsymbol{\chi_h}) \in \mathbb{RT}_k(\mathcal{T}_h), \tag{5.17}$$

where Π_h^k is the Raviart-Thomas interpolation operator introduced before (cf. (4.10) and (4.11)). We refer to (5.17) as a discrete Helmholtz decomposition of $\boldsymbol{\tau}_h$. Therefore, we can write

$$\boldsymbol{\tau}-\boldsymbol{\tau}_h \;=\; \boldsymbol{\tau}-\Pi_h^k(\boldsymbol{\zeta})-\underline{\mathbf{curl}}(\boldsymbol{\chi}_{\boldsymbol{h}}) \;=\; \boldsymbol{\zeta}-\Pi_h^k(\boldsymbol{\zeta})+\underline{\mathbf{curl}}(\boldsymbol{\chi}-\boldsymbol{\chi}_{\boldsymbol{h}})\,, \tag{5.18}$$

which, using (4.12) and the fact that $\mathbf{div}(\boldsymbol{\zeta})=\Delta\mathbf{z}=\mathbf{div}(\boldsymbol{\tau})$ in Ω, and denoting by $\mathbf{I}$ a generic identity operator, yields

$$\mathbf{div}(\boldsymbol{\tau}-\boldsymbol{\tau}_h) \;=\; \mathbf{div}\left(\boldsymbol{\zeta}-\Pi_h^k(\boldsymbol{\zeta})\right) \;=\; (\mathbf{I}-\mathcal{P}_h^k)(\mathbf{div}(\boldsymbol{\zeta})) \;=\; (\mathbf{I}-\mathcal{P}_h^k)(\mathbf{div}(\boldsymbol{\tau})). \tag{5.19}$$

Hence, according to (5.8), (5.9), and (5.10), and using the foregoing identities, we find that

$$\begin{aligned} E_1(\boldsymbol{\tau}-\boldsymbol{\tau}_h) \;=\; & \frac{1}{\alpha}\int_\Omega (\mathbf{f}+\mathbf{div}(\boldsymbol{\sigma}_h))\cdot(\mathbf{I}-\mathcal{P}_h^k)(\mathbf{div}(\boldsymbol{\tau})) \\ & + \int_\Omega \mathbf{t}_h : (\boldsymbol{\zeta}-\Pi_h^k(\boldsymbol{\zeta})) \;+\; \left\langle (\boldsymbol{\zeta}-\Pi_h^k(\boldsymbol{\zeta})\boldsymbol{\nu}, \boldsymbol{\xi}_h\right\rangle_{\Gamma_N} \\ & + \int_\Omega \mathbf{t}_h : \underline{\mathbf{curl}}(\boldsymbol{\chi}-\boldsymbol{\chi}_h) \;+\; \langle \underline{\mathbf{curl}}(\boldsymbol{\chi}-\boldsymbol{\chi}_h)\boldsymbol{\nu}, \boldsymbol{\xi}_h\rangle_{\Gamma_N}\,, \end{aligned} \tag{5.20}$$

and

$$E_2(\boldsymbol{\tau}-\boldsymbol{\tau}_h) \;=\; \kappa\int_\Omega (\boldsymbol{\sigma}_h^{\mathrm{d}}-\boldsymbol{\psi}(\mathbf{t}_h)) : \underline{\mathbf{curl}}(\boldsymbol{\chi}-\boldsymbol{\chi}_h) \;+\; \kappa\int_\Omega (\boldsymbol{\sigma}_h^{\mathrm{d}}-\boldsymbol{\psi}(\mathbf{t}_h)) : (\boldsymbol{\zeta}-\Pi_h^k(\boldsymbol{\zeta}))\,. \tag{5.21}$$

The following two lemmas provide the upper bounds for $|E_1(\boldsymbol{\tau}-\boldsymbol{\tau}_h)|$ and $|E_2(\boldsymbol{\tau}-\boldsymbol{\tau}_h)|$.

Lemma 5.3. *There exists $C>0$, independent of h and α, such that*

$$\begin{aligned} |E_1(\boldsymbol{\tau}-\boldsymbol{\tau}_h)| \;\leq\; & C\left\{\sum_{T\in\mathcal{T}_h}\left\{\frac{1}{\alpha^2}\|\mathbf{f}-\mathcal{P}_h^k(\mathbf{f})\|_{0,T}^2+h_T^2\,\|\mathbf{t}_h-\nabla\mathbf{u}_h\|_{0,T}^2+h_T^2\|\mathrm{curl}(\mathbf{t}_h)\|_{0,T}^2\right\}\right. \\ & + \sum_{e\in\mathcal{E}_h(\Omega)} h_e\|[\![\mathbf{t}_h\boldsymbol{\mathcal{s}}]\!]\|_{0,e}^2+\sum_{e\in\mathcal{E}_h(\Gamma_D)} h_e\|[\![\mathbf{t}_h\boldsymbol{\mathcal{s}}]\!]\|_{0,e}^2 \\ & \left. + \sum_{e\in\mathcal{E}_h(\Gamma_N)} h_e\left\{\left\|\mathbf{t}_h\boldsymbol{\mathcal{s}}+\frac{d\boldsymbol{\xi}_h}{d\boldsymbol{\mathcal{s}}}\right\|_{0,e}^2+\|\boldsymbol{\xi}_h+\mathbf{u}_h\|_{0,e}^2\right\}\right\}^{1/2}\|\boldsymbol{\tau}\|_{\mathbf{div},\Omega}. \end{aligned}$$

Proof. It follows exactly as in [9, Lemma 14], with $\mathbf{t}_h$ instead of $\frac{1}{\mu}\boldsymbol{\sigma}_h^{\mathrm{d}}$. The main tools employed are integration by parts, the Cauchy-Schwarz inequality, the approximation properties provided by Lemma 5.2, the identities (4.10) and (4.11) characterizing Π_h^k, the fact that the number of triangles in $\Delta(T)$ and $\Delta(e)$ are bounded, the approximation properties (4.14) and (4.16) (with $m=1$), and the estimate (5.16). We omit further details here. □

Lemma 5.4. *There exists $C>0$, independent of h, such that*

$$\begin{aligned} |E_2(\boldsymbol{\tau}-\boldsymbol{\tau}_h)| \;\leq\; & C\left\{\sum_{T\in\mathcal{T}_h}\left\{h_T^2\|\boldsymbol{\sigma}_h^{\mathrm{d}}-\boldsymbol{\psi}(\mathbf{t}_h)\|_{0,T}^2+h_T^2\|\mathrm{curl}(\boldsymbol{\sigma}_h^{\mathrm{d}}-\boldsymbol{\psi}(\mathbf{t}_h))\|_{0,T}^2\right.\right. \\ & \left.\left. + \sum_{e\in\mathcal{E}(T)} h_e\|[\![(\boldsymbol{\sigma}_h^{\mathrm{d}}-\boldsymbol{\psi}(\mathbf{t}_h))\boldsymbol{\mathcal{s}}]\!]\|_{0,e}^2\right\}\right\}^{1/2}\|\boldsymbol{\tau}\|_{\mathbf{div},\Omega}. \end{aligned}$$

Proof. It follows analogously to the proof of [13, Lemma 4.6], whose main ideas are taken from [12, Lemmas 4.3 and 4.4]. □

Having established the above bounds for $|E_1(\boldsymbol{\tau}-\boldsymbol{\tau}_h)|$ and $|E_2(\boldsymbol{\tau}-\boldsymbol{\tau}_h)|$, we conclude from Lemma 5.1 and (5.14) that there exists $C>0$, independent of h, such that

$$\|((\mathbf{t}-\mathbf{t}_h,\boldsymbol{\sigma}-\boldsymbol{\sigma}_h),\boldsymbol{\xi}-\boldsymbol{\xi}_h)\|_{H\times Q} \;\leq\; C\left\{\sum_{T\in\mathcal{T}_h}\widehat{\theta}_T^2+\|\mathbf{g}-\boldsymbol{\sigma}_h\boldsymbol{\nu}\|^2_{-1/2,\Gamma_N}\right\}^{1/2}, \tag{5.22}$$

where

$$\begin{aligned}\widehat{\theta}_T^2 \;:=\;& \frac{1}{\alpha^2}\|\mathbf{f}-\mathcal{P}_h^k(\mathbf{f})\|^2_{0,T}+h_T^2\,\|\mathbf{t}_h-\nabla\mathbf{u}_h\|^2_{0,T}+h_T^2\|\mathrm{curl}(\mathbf{t}_h)\|^2_{0,T}\\
&+\sum_{e\in\mathcal{E}(T)\cap\mathcal{E}_h(\Omega)}h_e\|[\![\mathbf{t}_h\boldsymbol{s}]\!]\|^2_{0,e}+\sum_{e\in\mathcal{E}(T)\cap\mathcal{E}_h(\Gamma_D)}h_e\|[\![\mathbf{t}_h\boldsymbol{s}]\!]\|^2_{0,e}\\
&+\sum_{e\in\mathcal{E}(T)\cap\mathcal{E}_h(\Gamma_N)}h_e\left\{\left\|\mathbf{t}_h\boldsymbol{s}+\frac{d\boldsymbol{\xi}_h}{d\boldsymbol{s}}\right\|^2_{0,e}+\|\boldsymbol{\xi}_h+\mathbf{u}_h\|^2_{0,e}\right\}\\
&+\|\boldsymbol{\sigma}_h^{\mathrm{d}}-\boldsymbol{\psi}(\mathbf{t}_h)\|^2_{0,T}+h_T^2\|\mathrm{curl}(\boldsymbol{\sigma}_h^{\mathrm{d}}-\boldsymbol{\psi}(\mathbf{t}_h))\|^2_{0,T}\\
&+\sum_{e\in\mathcal{E}(T)}h_e\|[\![(\boldsymbol{\sigma}_h^{\mathrm{d}}-\boldsymbol{\psi}(\mathbf{t}_h))\boldsymbol{s}]\!]\|^2_{0,e}.\end{aligned}$$

Now, in order to complete the upper bound for $\|((\mathbf{t}-\mathbf{t}_h,\boldsymbol{\sigma}-\boldsymbol{\sigma}_h),\boldsymbol{\xi}-\boldsymbol{\xi}_h)\|_{H\times Q}$ in terms of local error indicators, we need to estimate the Neumann residual $\|\mathbf{g}-\boldsymbol{\sigma}_h\boldsymbol{\nu}\|_{-1/2,\Gamma_N}$. Actually, this result was already proved in [9]. It is stated as follows.

Lemma 5.5. *Assume that the Neumann datum $\mathbf{g}\in\mathbf{L}^2(\Gamma_N)$. Then there exists $C>0$, independent of h, such that*

$$\|\mathbf{g}-\boldsymbol{\sigma}_h\boldsymbol{\nu}\|^2_{-1/2,\Gamma_N} \;\leq\; C\sum_{e\in\mathcal{E}_h(\Gamma_N)}h_e\|\mathbf{g}-\boldsymbol{\sigma}_h\boldsymbol{\nu}\|^2_{0,e}.$$

Proof. See [9, Lemma 15]. □

It is important to recall here, as remarked in [9, Remark after Lemma 15], that the regularity of the mesh $\mathcal{T}_h$ insures that the constant C in Lemma 5.5 is independent of h, whence the estimate provided there in terms of the computable local quantities $\|\mathbf{g}-\boldsymbol{\sigma}_h\boldsymbol{\nu}\|_{0,e}$ becomes suitable for the associated adaptive algorithm. Without this assumption, it would not make sense to apply this theorem, and we would have just to keep the expression $\|\mathbf{g}-\boldsymbol{\sigma}_h\boldsymbol{\nu}\|_{-1/2,\Gamma_N}$ in the a posteriori error estimator, thus rendering a non-local and hence useless quantity for adaptivity.

Then, as a consequence of Lemmas 5.1 and 5.5, together with the estimate (5.22), we conclude that there exists $C>0$, independent of h, such that

$$\|((\mathbf{t}-\mathbf{t}_h,\boldsymbol{\sigma}-\boldsymbol{\sigma}_h),\boldsymbol{\xi}-\boldsymbol{\xi}_h)\|_{H\times Q} \;\leq\; C\boldsymbol{\theta}, \tag{5.23}$$

where $\boldsymbol{\theta}$ is the global a posteriori error estimator defined by (5.3) and (5.1).

On the other hand, the upper bound for $\|\mathbf{u}-\mathbf{u}_h\|_{0,\Omega}$ is quite straightforward from the definition of $\mathbf{u}$ and $\mathbf{u}_h$. Indeed, recalling that

$$\mathbf{u} \;=\; \frac{1}{\alpha}\{\mathbf{f}+\mathbf{div}(\boldsymbol{\sigma})\} \quad\text{ and }\quad \mathbf{u}_h \;=\; \frac{1}{\alpha}\left\{\mathcal{P}_h^k(\mathbf{f})+\mathbf{div}(\boldsymbol{\sigma}_h)\right\},$$

we easily obtain

$$\|\mathbf{u}-\mathbf{u}_h\|_{0,\Omega} \;\leq\; \frac{1}{\alpha}\left\{\|\mathbf{f}-\mathcal{P}_h^k(\mathbf{f})\|_{0,\Omega}+\|\boldsymbol{\sigma}-\boldsymbol{\sigma}_h\|_{\mathbf{div},\Omega}\right\}. \tag{5.24}$$

Finally, from (5.24) and (5.23) we have that there exists $C_{\mathtt{rel}}>0$, independent of h, such that

$$\|\mathbf{u}-\mathbf{u}_h\|_{0,\Omega} \;+\; \|((\mathbf{t}-\mathbf{t}_h,\boldsymbol{\sigma}-\boldsymbol{\sigma}_h),\boldsymbol{\xi}-\boldsymbol{\xi}_h)\|_{H\times Q} \;\leq\; C_{\mathtt{rel}}\boldsymbol{\theta},$$

which proves the reliability of the estimator $\boldsymbol{\theta}$.

5.3 Efficiency

In this section we prove the efficiency of our a posteriori error estimator $\boldsymbol{\theta}$ (lower bound in (5.4)). In other words, we derive suitable upper bounds for the eleven terms defining the local error indicator θ_T^2 (cf. (5.1)). We first notice, using the definitions of $\mathbf{u}$ (cf. (3.7)) and $\mathbf{u}_h$ (cf. (5.2)), that

$$\|\mathbf{f}-\mathcal{P}_h^k(\mathbf{f})\|_{0,T}^2 \;\leq\; 2\alpha^2\|\mathbf{u}-\mathbf{u}_h\|_{0,T}^2 \;+\; 2\|\mathbf{div}\big(\boldsymbol{\sigma}-\boldsymbol{\sigma}_h\big)\|_{0,T}^2. \tag{5.25}$$

On the other hand, we notice that the converse of the derivation of (3.9) from (2.5) holds true. Indeed, it is easy to show, applying integration by parts backwardly and using appropriate test functions, that the unique solution $((\mathbf{t},\boldsymbol{\sigma}),\boldsymbol{\xi})\in H\times Q$ of (3.9) solves the original problem (2.5). Then, using that $\boldsymbol{\sigma}^{\mathrm{d}}=\boldsymbol{\psi}(\mathbf{t})$ in Ω and applying the Lipschitz-continuity of $\mathbb{A}$ (cf. Lemma 3.2), but restricted to the triangle $T\in\mathcal{T}_h$ instead of Ω, we deduce that

$$\begin{aligned}\|\boldsymbol{\sigma}_h^{\mathrm{d}}-\boldsymbol{\psi}(\mathbf{t}_h)\|_{0,T} &\leq \|(\boldsymbol{\sigma}-\boldsymbol{\sigma}_h)^{\mathrm{d}}\|_{0,T}+\|\mu(|\mathbf{t}|)\mathbf{t}-\mu(|\mathbf{t}_h|)\mathbf{t}_h\|_{0,T},\\ &\leq \|\boldsymbol{\sigma}-\boldsymbol{\sigma}_h\|_{0,T}+\gamma_0\|\mathbf{t}-\mathbf{t}_h\|_{0,T}.\end{aligned} \tag{5.26}$$

Next, in order to bound the terms involving the mesh parameters h_T and h_e, we make use of the results and estimates available for the corresponding linear case (cf. [9, Section 4.3]). The techniques applied there are based on triangle-bubble and edge-bubble functions, extension operators, and discrete trace and inverse inequalities. For further details on these tools we refer particularly to [9, Lemmas 16 and 17, and eq. (67)].

Hence, the estimates of the remaining nine terms defining θ_T^2 (cf. (5.1)) are given as follows.

Lemma 5.6. *There exist $C_1,C_2>0$, independent of h, such that*

$$h_T^2\|\mathrm{curl}(\mathbf{t}_h)\|_{0,T}^2 \;\leq\; C_1\|\mathbf{t}-\mathbf{t}_h\|_{0,T}^2 \quad\forall\, T\in\mathcal{T}_h,$$

and

$$h_e\|[\![\mathbf{t}_h\boldsymbol{s}_e]\!]\|_{0,e}^2 \;\leq\; C_2\|\mathbf{t}-\mathbf{t}_h\|_{0,\omega_e}^2 \quad\forall\, e\in\mathcal{E}_h(\Omega),$$

where $\omega_e:=\cup\{\,T\in\mathcal{T}_h\;:\;e\in\mathcal{E}(T)\}$.

Proof. It follows as in the proof of [9, Lemma 19] by replacing there $\frac{1}{\mu}\boldsymbol{\sigma}_h$ by $\mathbf{t}_h$. □

Lemma 5.7. *There exists $C_3>0$, independent of h, such that*

$$h_T^2\,\|\mathbf{t}_h-\nabla\mathbf{u}_h\|_{0,T}^2 \;\leq\; C_3\left\{\|\mathbf{u}-\mathbf{u}_h\|_{0,T}^2+h_T^2\|\mathbf{t}-\mathbf{t}_h\|_{0,T}^2\right\} \quad\forall\, T\in\mathcal{T}_h\,.$$

Proof. Similarly to the previous lemma, it follows by replacing $\frac{1}{\mu}\boldsymbol{\sigma}_h^{\mathrm{d}}$ by $\mathbf{t}_h$ in the proof of [9, Lemma 20], and then using that $\mathbf{t}=\nabla\mathbf{u}$ in Ω. □

Lemma 5.8. *There exists $C_4 > 0$, independent of h, such that for each $e \in \mathcal{E}_h(\Gamma_D)$ there holds*

$$h_e \, \|[\mathbf{t}_h \boldsymbol{s}]\|_{0,e}^2 \;\leq\; C_4 \|\mathbf{t} - \mathbf{t}_h\|_{0,T_e}^2,$$

where T_e is the triangle of $\mathcal{T}_h$ having e as an edge.

Proof. Similarly to the previous lemma, it follows by replacing $\frac{1}{\mu}\boldsymbol{\sigma}_h^{\mathrm{d}}$ by $\mathbf{t}_h$ in the proof of [9, Lemma 21], and then using that $\mathbf{t} = \nabla \mathbf{u}$ in Ω and $\mathbf{u} = \mathbf{0}$ in Γ_D. □

Lemma 5.9. *Assume that Σ_h is quasi-uniform. Then there exists $C_5 > 0$, independent of h, such that*

$$\sum_{e \in \mathcal{E}_h(\Gamma_N)} h_e \left\| \mathbf{t}_h \boldsymbol{s} + \frac{d\boldsymbol{\xi}_h}{d\boldsymbol{s}} \right\|_{0,e}^2 \;\leq\; C_5 \left\{ \sum_{e \in \mathcal{E}_h(\Gamma_N)} \|\mathbf{t} - \mathbf{t}_h\|_{0,T_e}^2 + \|\boldsymbol{\xi} - \boldsymbol{\xi}_h\|_{0;1/2,\Gamma_N}^2 \right\},$$

where, given $e \in \mathcal{E}_h(\Gamma_N)$, T_e is the triangle of $\mathcal{T}_h$ having e as edge.

Proof. It follows as in the proof of [9, Lemma 22], by replacing there $\frac{1}{\mu}\boldsymbol{\sigma}_h^{\mathrm{d}}$ by $\mathbf{t}_h$, and then using that $\mathbf{t} = \nabla \mathbf{u}$ in Ω. □

Note, as in [9], that the estimate provided by Lemma 5.9 is the only nonlocal bound of the present efficiency analysis. In addition, this lemma is the only one needing to assume that Σ_h is quasi-uniform. However, under an additional local regularity assumption on $\boldsymbol{\xi}$, but without assuming any quasi-uniformity condition, we are able to prove the following local bound.

Lemma 5.10. *Assume that $\boldsymbol{\xi}|_e \in \mathbf{H}^1(e)$ for each $e \in \mathcal{E}_h(\Gamma_N)$. Then there exists $\widetilde{C}_5 > 0$, independent of h, such that for each $e \in \mathcal{E}_h(\Gamma_N)$ there holds*

$$h_e \left\| \mathbf{t}_h \boldsymbol{s} + \frac{d\boldsymbol{\xi}_h}{d\boldsymbol{s}} \right\|_{0,e}^2 \;\leq\; \widetilde{C}_5 \left\{ \|\mathbf{t} - \mathbf{t}_h\|_{0,T_e}^2 + h_e \left\| \frac{d}{d\boldsymbol{s}} (\boldsymbol{\xi} - \boldsymbol{\xi}_h) \right\|_{0,e}^2 \right\},$$

where T_e is the triangle of $\mathcal{T}_h$ having e as edge.

Proof. It suffices to replace again $\frac{1}{\mu}\boldsymbol{\sigma}_h^{\mathrm{d}}$ by $\mathbf{t}_h$ in [9, Lemma 23]. □

Next, we continue with the bound for the boundary terms on each $e \in \mathcal{E}_h(\Gamma_N)$.

Lemma 5.11. *There exists $C_6 > 0$, independent of h, such that for each $e \in \mathcal{E}_h(\Gamma_N)$ there holds*

$$h_e \|\boldsymbol{\xi}_h + \mathbf{u}_h\|_{0,e}^2 \;\leq\; C_6 \Big\{ h_e \|\boldsymbol{\xi} - \boldsymbol{\xi}_h\|_{0,e}^2 + \|\mathbf{u} - \mathbf{u}_h\|_{0,T_e}^2 + h_{T_e}^2 \|\mathbf{t} - \mathbf{t}_h\|_{0,T_e}^2 \Big\},$$

where T_e is the triangle of $\mathcal{T}_h$ having e as an edge.

Proof. It follows as in the proof of [9, Lemma 24], using that $\boldsymbol{\xi} = -\mathbf{u}$ on Γ_N, $\mathbf{t} = \nabla \mathbf{u}$ in Ω and Lemma 5.7. □

Lemma 5.12. *Assume that $\mathbf{g}$ is piecewise polynomial. Then there exists $C_7 > 0$, independent of h, such that for each $e \in \mathcal{E}_h(\Gamma_N)$ there holds*

$$h_e \|\mathbf{g} - \boldsymbol{\sigma}_h \boldsymbol{\nu}\|_{0,e}^2 \;\leq\; C_7 \Big\{ \|\boldsymbol{\sigma} - \boldsymbol{\sigma}_h\|_{0,T_e}^2 + h_{T_e}^2 \|\mathbf{div}(\boldsymbol{\sigma} - \boldsymbol{\sigma}_h)\|_{0,T_e}^2 \Big\}, \tag{5.27}$$

where T_e is the triangle of $\mathcal{T}_h$ having e as an edge.

Proof. It follows as in the proof of [9, Lemma 25], using that $\mathbf{g} = \boldsymbol{\sigma}\boldsymbol{\nu}$ on Γ_N. □

If $\mathbf{g}$ were not piecewise polynomial but sufficiently smooth, then higher order terms given by the errors arising from suitable polynomial approximations would appear in (5.27). This explains the eventual expression *h.o.t.* in (5.4).

Finally, for the efficiency of $\boldsymbol{\theta}$ it only remains to provide upper bounds for the two terms completing the definition of the local error indicator θ_T^2 (cf. (5.1)), which is established in the following lemma.

Lemma 5.13. *There exist $C_8, C_9 > 0$, independent of h, such that*

$$h_T^2 \|\mathrm{curl}(\boldsymbol{\sigma}_h^{\mathrm{d}} - \boldsymbol{\psi}(\mathbf{t}_h))\|_{0,T}^2 \;\leq\; C_8 \left\{ \|\mathbf{t} - \mathbf{t}_h\|_{0,T}^2 + \|\boldsymbol{\sigma} - \boldsymbol{\sigma}_h\|_{0,T}^2 \right\} \quad \forall\, T \in \mathcal{T}_h,$$

and

$$h_e \|[\![(\boldsymbol{\sigma}_h^{\mathrm{d}} - \boldsymbol{\psi}(\mathbf{t}_h))\boldsymbol{s}]\!]\|_{0,e}^2 \;\leq\; C_9 \left\{ \|\mathbf{t} - \mathbf{t}_h\|_{0,\omega_e}^2 + \|\boldsymbol{\sigma} - \boldsymbol{\sigma}_h\|_{0,\omega_e}^2 \right\} \quad \forall\, e \in \mathcal{E}_h\,.$$

Proof. It follows analogously to the proof of [13, Lemma 4.11], which applies [9, Lemma 18] to $\boldsymbol{\rho}_h = \boldsymbol{\sigma}_h^{\mathrm{d}} - \boldsymbol{\psi}(\mathbf{t}_h)$ and $\boldsymbol{\rho} = \boldsymbol{\sigma}^{\mathrm{d}} - \boldsymbol{\psi}(\mathbf{t})$ in Ω, and then uses the Lipschitz-continuity of $\mathbb{A}$ (cf. Lemma 3.2) restricted to T and ω_e. □

Consequently, the efficiency of $\boldsymbol{\theta}$ follows straightforwardly from estimates (5.25) and (5.26), together with Lemmas 5.7 throughout 5.13, after summing up over $T \in \mathcal{T}_h$.

6 Numerical results

In this section, we present four numerical examples demonstrating a good performance of the augmented mixed finite element scheme (4.5), confirming the reliability and efficiency of the a posteriori error estimator $\boldsymbol{\theta}$ derived in Section 5, and showing the behaviour of the associated adaptive algorithm. In all the computations we consider the specific finite element subspaces H_h and Q_h given respectively by (4.1) and (4.3), with $k \in \{0, 1, 2\}$ and $\Sigma_{\tilde{h}} := \Sigma_{2h}$. We begin by introducing additional notations. In what follows N stands for the total number of degrees of freedom (unknowns) of (4.5), that is,

$$\begin{aligned} N \;:=\; & 2(k+1) \times (\#\text{ of edges in } \mathcal{T}_h) \;+\; \{3d_k + 2k(k+2)\} \times (\#\text{ of elements in } \mathcal{T}_h) \\ & + 2\left\{(k+1) \times (\#\text{ of edges in } \Sigma_{\tilde{h}}) + 1\right\}, \end{aligned}$$

with $d_k := \frac{1}{2}(k+1)(k+2)$. Also, the individual and total errors are defined by

$$\begin{aligned} \mathtt{e}(\mathbf{t}) &:= \|\mathbf{t} - \mathbf{t}_h\|_{0,\Omega}, & \mathtt{e}(\boldsymbol{\sigma}) &:= \|\boldsymbol{\sigma} - \boldsymbol{\sigma}_h\|_{\mathbf{div},\Omega}, \\ \mathtt{e}(\boldsymbol{\xi}) &:= \|\boldsymbol{\xi} - \boldsymbol{\xi}_h\|_{0;1/2,\Gamma_N}, & \mathtt{e}(\mathbf{u}) &:= \|\mathbf{u} - \mathbf{u}_h\|_{0,\Omega}, \\ \mathtt{e}(\mathbf{t},\boldsymbol{\sigma},\boldsymbol{\xi}) &:= \left\{[\mathtt{e}(\mathbf{t})]^2 + [\mathtt{e}(\boldsymbol{\sigma})]^2 + [\mathtt{e}(\boldsymbol{\xi})]^2\right\}^{1/2}, & \mathtt{e}(p) &:= \|p - p_h\|_{0,\Omega}, \end{aligned}$$

$$\mathtt{e}(\mathbf{t},\boldsymbol{\sigma},\boldsymbol{\xi},\mathbf{u}) := \left\{[\mathtt{e}(\mathbf{t})]^2 + [\mathtt{e}(\boldsymbol{\sigma})]^2 + [\mathtt{e}(\boldsymbol{\xi})]^2 + [\mathtt{e}(\mathbf{u})]^2\right\}^{1/2},$$

where p_h and $\mathbf{u}_h$ are computed by the postprocessing formulae (4.6) and (5.2), whereas the effectivity index with respect to $\boldsymbol{\theta}$ is given by

$$\mathtt{eff}(\boldsymbol{\theta}) := \mathtt{e}(\mathbf{t},\boldsymbol{\sigma},\boldsymbol{\xi},\mathbf{u}) \,/\, \boldsymbol{\theta}.$$

Then, we define the experimental rates of convergence

$$\mathtt{r}(\mathbf{t}) := \frac{\log(\mathtt{e}(\mathbf{t})/\mathtt{e}'(\mathbf{t}))}{\log(h/h')} \qquad \mathtt{r}(\boldsymbol{\sigma}) := \frac{\log(\mathtt{e}(\boldsymbol{\sigma})/\mathtt{e}'(\boldsymbol{\sigma}))}{\log(h/h')},$$

$$\mathtt{r}(\boldsymbol{\xi}) := \frac{\log(\mathtt{e}(\boldsymbol{\xi})/\mathtt{e}'(\boldsymbol{\xi}))}{\log(h/h')}, \quad \mathtt{r}(\mathbf{t},\boldsymbol{\sigma},\boldsymbol{\xi}) := \frac{\log(\mathtt{e}(\mathbf{t},\boldsymbol{\sigma},\boldsymbol{\xi})/\mathtt{e}'(\mathbf{t},\boldsymbol{\sigma},\boldsymbol{\xi}))}{\log(h/h')},$$

and similarly for $\mathtt{r}(p)$ and $\mathtt{r}(\mathbf{u})$, where $\mathtt{e}$ and $\mathtt{e}'$ denote the corresponding errors for two consecutive triangulations with mesh sizes h and h', respectively. Nevertheless, when the adaptive algorithm is applied (see details below), the expression $\log(h/h')$ appearing in the computation of the above rates is replaced by $-\frac{1}{2}\log(N/N')$, where N and N' denote the corresponding degrees of freedom of each triangulation.

The numerical results presented below were obtained using a C^{++} code. The corresponding nonlinear algebraic systems arising from (3.9) are solved by the Newton-Raphson method with a tolerance of 10^{-6} and taking the solution of the associated linear Brinkman problem ($\mu = 1$) as initial iteration for the quasi-uniform scheme. In all the examples no more than four iterations were required to achive the given tolerance. In turn, the linear systems were solved using the Conjugate Gradient method as main solver, and applying a stopping criterion determined by a relative tolerance of 10^{-10}.

The examples to be considered in this section, some of them taken from [9], are described next. Example 1 and 2 (linear and nonlinear, respectively) are employed to illustrate the performance of the augmented mixed finite element scheme (4.5) and to confirm the reliability and efficiency of the a posteriori error estimator $\boldsymbol{\theta}$. Examples 3 and 4 are utilized to show the behaviour of the associated adaptive algorithm, which applies the following procedure:

(1) Start with a coarse mesh $\mathcal{T}_h$.

(2) Solve the linear version of the discrete problem (4.5), in order to obtain an initial guest $\mathbf{x}_0$, for the Newton iterations.

(3) Solve the discrete problem (4.5) for the actual mesh $\mathcal{T}_h$, with the actual initial guest $\mathbf{x}_0$.

(4) Compute θ_T (cf. (5.1)) for each triangle $T \in \mathcal{T}_h$,

(5) Evaluate stopping criterion ($\boldsymbol{\theta} \leq$ given tolerance) and decide to finish or go to next step.

(6) Use *red-green-blue* procedure (cf. [24]) to refine each $T' \in \mathcal{T}_h$ whose indicator $\theta_{T'}$ satisfies

$$\theta_{T'} \geq \frac{1}{2}\max\{\theta_T : T \in \mathcal{T}_h\}.$$

(7) Use the solution given by step 3 and the new mesh to interpolate a new initial guess $\widetilde{\mathbf{x}}_0$ and then replace $\mathbf{x}_0$ by $\widetilde{\mathbf{x}}_0$.

(8) Define the new mesh as actual mesh $\mathcal{T}_h$ and go to step 3.

For Example 1 we take $\mu = 1$ and for the remaining three examples we consider the nonlinear function $\mu : R^+ \to R^+$ given by the Carreau law

$$\mu(t) := \mu_0 + \mu_1(1+t^2)^{(\beta-2)/2} \quad \forall\, t \in R^+,$$

with $\mu_0 = \mu_1 = 0.5$ and $\beta = 1.5$. It is easy to check that the assumptions (2.2) and (2.3) are satisfied with

$$\gamma_0 = \mu_0 + \mu_1\left\{\frac{|\beta-2|}{2}+1\right\} \quad \text{and} \quad \alpha_0 = \mu_0.$$

Hence, for the implementation of the augmented scheme (4.5) we use the stabilization parameter $\kappa = \frac{\alpha_0}{\gamma_0^2}$, which certainly satisfies the required hypothesis $\kappa \in \left(0, \frac{2\alpha_0}{\gamma_0^2}\right)$.

In Example 1 we consider $\Omega = (0,1)^2$, $\Gamma_D = \big\{(0, x_2) \in R^2 \ : \ 0 \leq x_2 \leq 1\big\}$, $\Gamma_N = \Gamma \setminus \bar{\Gamma}_D$, $\alpha = 1$, and choose the data $\mathbf{f}$ and $\mathbf{g}$ so that the exact solution is given for each $\mathbf{x} := (x_1, x_2)^{\mathrm{t}} \in \Omega$ by

$$\mathbf{u}(\mathbf{x}) \ = \ \begin{pmatrix} \sin^2(4x_1)\ \cos(4x_2)\ \sin(4x_2) \\ \sin(4x_1)\ \cos^2(4x_2)\ \cos(4x_1) \end{pmatrix}$$

and

$$p(\mathbf{x}) \ = \ \cos(4x_1)\ \cos(4x_2)\ \exp(-x_1).$$

It is easy to check that $\mathbf{u}$ is divergence free, and $(\mathbf{u}, p)$ is regular in the whole domain Ω.

In Example 2 we consider $\Omega = (0,1)^2$, $\Gamma_D = \big\{(w, 0), (0, w) \in R^2 \ : \ 0 \leq w \leq 1\big\}$, $\Gamma_N = \Gamma \setminus \bar{\Gamma}_D$, $\alpha = \frac{1}{2\pi}$, and choose the data $\mathbf{f}$ and $\mathbf{g}$ so that the exact solution is given for each $\mathbf{x} := (x_1, x_2)^{\mathrm{t}} \in \Omega$ by

$$\mathbf{u}(\mathbf{x}) \ = \ \begin{pmatrix} (1 + x_1 - \exp(x_1))\ (1 - \cos(x_2)) \\ (\exp(x_1) - 1)\ (x_2 - \sin(x_2)) \end{pmatrix}$$

and

$$p(\mathbf{x}) \ = \ \frac{1}{2}\ \exp(2\pi x_1).$$

Note that $\mathbf{u}$ is divergence free and $(\mathbf{u}, p)$ is regular in the whole domain Ω.

In Example 3 we consider $\Omega = \,]-1,1[^2 \backslash [0,1]^2$, $\Gamma_D = \{(-1, x_2) \in R^2 : -1 \leq x_2 \leq 1\}$, $\Gamma_N = \Gamma \setminus \bar{\Gamma}_D$, $\alpha = 1$, and choose $\mathbf{f}$ and $\mathbf{g}$ so that the exact solution is given for each $\mathbf{x} := (x_1, x_2)^{\mathrm{t}} \in \Omega$ by

$$\mathbf{u}(\mathbf{x}) \ = \ \mathbf{curl}\left((x_1 + 1)^2 \sqrt{(x_1 - 0.1)^2 \ + \ (x_2 - 0.1)^2}\right)$$

and

$$p(\mathbf{x}) \ = \ \frac{1}{x_2 \ + \ 1.1}.$$

Note that Ω is an L-shaped domain and that $\mathbf{u}$ and p are singular at $(0.1, 0.1)$ and along the line $x_2 = -1.1$, respectively. Hence, we should expect regions of high gradients around the origin, which is the middle corner of the L, and along the line $x_2 = -1$.

Finally, in Example 4 we consider $\Omega = \,]-1,1[^2 \backslash \left([-1, -0.25] \times [-1, 0.5] \cup [0.25, 1] \times [-1, 0.5]\right)$, $\Gamma_D = \{(x_1, 1) \in R^2 : -1 \leq x_1 \leq 1\}$, $\Gamma_N = \Gamma \setminus \bar{\Gamma}_D$, $\alpha = 10$, and choose the data $\mathbf{f}$ and $\mathbf{g}$ so that the exact solution is given for each $\mathbf{x} := (x_1, x_2)^{\mathrm{t}} \in \Omega$ by

$$\begin{aligned} \mathbf{u}(\mathbf{x}) \ = \ \mathbf{curl}\Big((x_2 - 1)^2 \Big\{ & \sqrt{(x_1 + 0.3)^2 \ + \ (x_2 - 0.45)^2} \\ & + \ \sqrt{(x_1 - 0.3)^2 \ + \ (x_2 - 0.45)^2} \Big\}\Big) \end{aligned}$$

and

$$p(\mathbf{x}) \ = \ \frac{1}{x_2 \ + \ 1.1}.$$

Note that Ω is a T-shaped domain and that $\mathbf{u}$ and p are singular at $(-0.3, 0.45)$ and $(0.3, 0.45)$, and along the line $x_2 = -1.1$, respectively. Hence, similarly to Example 3, we should expect regions of high gradients around $(-0.25, 0.5)$ and $(0.25, 0.5)$, which are the middle corners of the T, and along the line $x_2 = -1$.

In Tables 6.1, 6.2, 6.3, and 6.4, we summarize the convergence history of the augmented mixed finite element scheme (3.9) as applied to Example 1 and 2, for a sequence of quasi-uniform triangulations

of each domain. We notice there that the rate of convergence $O(h^{k+1})$ predicted by Theorem 4.2 (when $s = k + 1$) is attained by all the unknowns, including the postprocessed $\mathbf{u}$ and p (cf. Tables 6.2 and 6.4). In particular, as observed in the ninth column of Tables 6.1 and 6.3, the convergence of $\boldsymbol{\xi}_h$ is a bit faster than expected, which could correspond to either a superconvergence phenomenon or a special feature of these examples. A similar phenomenon holds for the variable $\mathbf{u}$ in Table 6.4 for $k \geq 1$. We also remark the good behaviour of the a posteriori error estimator $\boldsymbol{\theta}$ in this case. In particular, in Table 6.1, we see that the effectivity index $\texttt{eff}(\boldsymbol{\theta})$ remains always in a neighborhood of 0.905 for $k = 0$, which illustrates the reliability and efficiency result provided by Theorem 5.1.

Next, in Tables 6.5, 6.6, 6.7, and 6.8, we provide the convergence history of the quasi-uniform and adaptive schemes as applied to Examples 3 and 4. The stopping criterion in both adaptive refinements is $\boldsymbol{\theta} \leq 0.2$. We observe here, as expected, that the errors of the adaptive methods decrease faster than those obtained by the quasi-uniform ones. This fact is better illustrated in Figures. 6.1 and 6.3 where we display the errors $\texttt{e}(\mathbf{t}, \boldsymbol{\sigma}, \boldsymbol{\xi})$ vs. the degrees of freedom N for both refinements. In addition, the effectivity indices remain again bounded from above and below, which confirms the reliability and efficiency of $\boldsymbol{\theta}$ for the associated adaptive algorithm as well. Some intermediate meshes obtained with this procedure are displayed in Figures 6.2 and 6.4. Notice here that the adapted meshes concentrate the refinements around the origin and the line $x_2 = -1$ in Example 3, and around the points $(-0.25, 0.5)$ and $(0.25, 0.5)$ and the line $x_2 = -1$ in Example 4, which means that the method is in fact able to recognize the regions with high gradients of the solutions. Finally, in order to illustrate the accurateness of the adaptive scheme, in Figures 6.5, 6.6, 6.7, and 6.8, we display some components of the solutions for both examples. For the field unknowns, the approximate ones are placed at the left side whereas the exact ones are placed at the right side. In turn, the components of the boundary unknown $\boldsymbol{\xi}$ are depicted along straight lines beginning at the points $(-1, -1)$ and $(-1, 1)$ for the L-shaped and T-shaped domains, respectively, and then continuing counterclockwise. This gives the 1D graphs in which the two approximate components of $\boldsymbol{\xi}$ are identified by red bullets whereas the exact ones are identified by continuous blue lines.

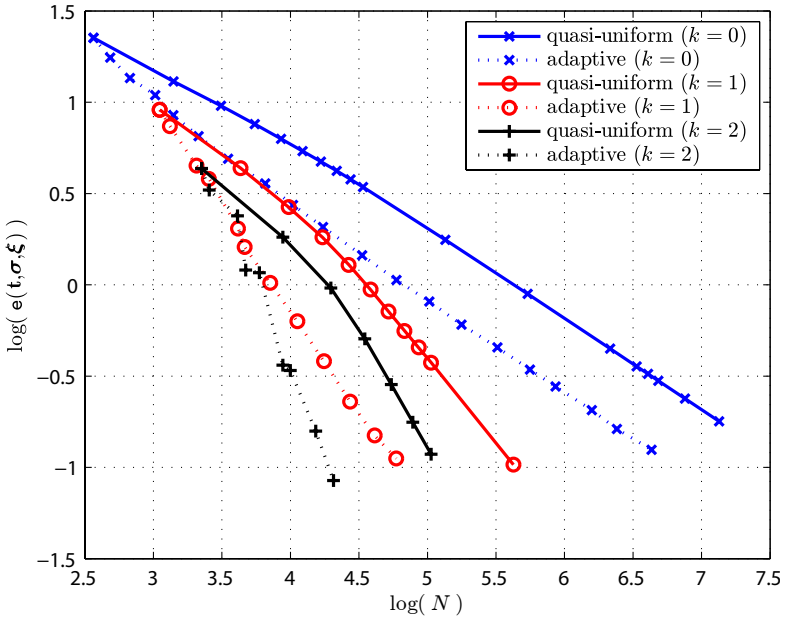

Figure 6.1: Example 3, $\texttt{e}(\mathbf{t}, \boldsymbol{\sigma}, \boldsymbol{\xi})$ vs. N.

k	h	N	$\mathtt{e}(\mathbf{t})$	$\mathtt{r}(\mathbf{t})$	$\mathtt{e}(\boldsymbol{\sigma})$	$\mathtt{r}(\boldsymbol{\sigma})$	$\mathtt{e}(\boldsymbol{\xi})$	$\mathtt{r}(\boldsymbol{\xi})$	$\mathtt{e}(\mathbf{t},\boldsymbol{\sigma},\boldsymbol{\xi})$	$\mathtt{r}(\mathbf{t},\boldsymbol{\sigma},\boldsymbol{\xi})$	$\mathtt{eff}(\boldsymbol{\theta})$
	1/16	7282	3.62e-1	−−	2.98e-0	−−	7.56e-2	−−	3.01e-0	−−	0.9047
	1/20	11342	2.87e-1	1.04	2.39e-0	1.00	4.49e-2	2.34	2.41e-0	1.00	0.9049
	1/24	16298	2.39e-1	1.02	1.99e-0	1.00	2.99e-2	2.24	2.01e-0	1.00	0.9050
	1/28	22150	2.04e-1	1.01	1.71e-0	1.00	2.13e-2	2.18	1.72e-0	1.00	0.9051
0	1/32	28898	1.78e-1	1.01	1.49e-0	1.00	1.60e-2	2.14	1.50e-0	1.00	0.9052
	1/36	36542	1.58e-1	1.01	1.33e-0	1.00	1.25e-2	2.11	1.34e-0	1.00	0.9052
	1/48	64850	1.19e-1	1.00	9.96e-1	1.00	6.86e-3	2.08	1.00e-0	1.00	0.9053
	1/64	115138	8.90e-2	1.00	7.47e-1	1.00	3.80e-3	2.05	7.53e-1	1.00	0.9053
	1/96	258722	5.93e-2	1.00	4.98e-1	1.00	1.67e-3	2.03	5.02e-1	1.00	0.9054
	1/128	459650	4.45e-2	1.00	3.74e-1	1.00	9.33e-4	2.02	3.76e-1	1.00	0.9054
	1/16	22754	2.78e-2	−−	1.78e-1	−−	8.13e-3	−−	1.80e-1	−−	0.7826
	1/20	35482	1.72e-2	2.17	1.14e-1	2.01	4.38e-3	2.78	1.15e-1	2.01	0.7899
	1/24	51026	1.15e-2	2.19	7.90e-2	2.01	2.61e-3	2.84	7.99e-2	2.01	0.7948
	1/28	69386	8.22e-3	2.19	5.80e-2	2.01	1.68e-3	2.88	5.86e-2	2.01	0.7982
1	1/32	90562	6.14e-3	2.19	4.44e-2	2.01	1.14e-3	2.90	4.48e-2	2.01	0.8006
	1/36	114554	4.75e-3	2.18	3.50e-2	2.01	8.06e-4	2.92	3.54e-2	2.01	0.8024
	1/48	203426	2.54e-3	2.17	1.97e-2	2.00	3.47e-4	2.93	1.98e-2	2.01	0.8058
	1/64	361346	1.38e-3	2.14	1.11e-2	2.00	1.53e-4	2.84	1.11e-2	2.01	0.8082
	1/96	812354	5.86e-4	2.11	4.91e-3	2.00	4.82e-5	2.85	4.94e-3	2.00	0.8102
	1/128	1443586	3.20e-4	2.11	2.76e-3	2.00	2.12e-5	2.85	2.78e-3	2.00	0.8112
	1/16	46418	1.40e-3	−−	7.33e-3	−−	3.48e-4	−−	7.47e-3	−−	0.5903
	1/20	72422	6.53e-4	3.42	3.73e-3	3.03	1.48e-4	3.82	3.79e-3	3.04	0.6041
	1/24	104186	3.50e-4	3.41	2.15e-3	3.02	6.84e-5	4.24	2.18e-3	3.04	0.6182
	1/28	141710	2.08e-4	3.37	1.35e-3	3.02	3.47e-5	4.41	1.37e-3	3.03	0.6295
2	1/32	184994	1.34e-4	3.32	9.02e-4	3.02	2.01e-5	4.06	9.12e-4	3.02	0.6376
	1/36	234038	9.08e-5	3.29	6.33e-4	3.01	1.25e-5	4.05	6.39e-4	3.02	0.6442
	1/48	415730	3.57e-5	3.25	2.66e-4	3.01	4.02e-6	3.94	2.69e-4	3.02	0.6581
	1/64	738626	1.41e-5	3.22	1.12e-4	3.01	1.30e-6	3.93	1.13e-4	3.01	0.6668
	1/96	1660898	3.83e-6	3.22	3.29e-5	3.02	2.63e-7	3.94	3.31e-5	3.02	0.6669
	1/128	2951810	1.52e-6	3.22	1.38e-5	3.02	8.48e-8	3.94	1.39e-5	3.02	0.6669

Table 6.1: Example 1, quasi-uniform scheme.

k	h	N	$\mathtt{e}(\mathbf{u})$	$\mathtt{r}(\mathbf{u})$	$\mathtt{e}(\mathtt{p})$	$\mathtt{r}(\mathtt{p})$
0	1/16	7282	2.93e-2	−−	1.47e-1	−−
	1/20	11342	2.35e-2	1.00	1.15e-1	1.10
	1/24	16298	1.95e-2	1.00	9.50e-2	1.06
	1/28	22150	1.68e-2	1.00	8.10e-2	1.04
	1/32	28898	1.47e-2	1.00	7.06e-2	1.03
	1/36	36542	1.30e-2	1.00	6.26e-2	1.02
	1/48	64850	9.78e-3	1.00	4.68e-2	1.01
	1/64	115138	7.33e-3	1.00	3.51e-2	1.01
	1/96	258722	4.89e-3	1.00	2.33e-2	1.00
	1/128	459650	3.67e-3	1.00	1.75e-2	1.00
1	1/16	22754	1.66e-3	−−	1.57e-2	−−
	1/20	35482	1.05e-3	2.03	9.19e-3	2.40
	1/24	51026	7.29e-4	2.02	5.92e-3	2.41
	1/28	69386	5.35e-4	2.01	4.09e-3	2.40
	1/32	90562	4.09e-4	2.01	2.97e-3	2.39
	1/36	114554	3.23e-4	2.01	2.25e-3	2.36
	1/48	203426	1.82e-4	2.00	1.15e-3	2.33
	1/64	361346	1.03e-4	1.98	6.00e-4	2.26
	1/96	812354	4.60e-5	1.98	2.43e-4	2.23
	1/128	1443586	2.59e-5	2.00	1.32e-4	2.12
2	1/16	46418	6.42e-5	−−	9.95e-4	−−
	1/20	72422	3.36e-5	2.91	4.55e-4	3.51
	1/24	104186	1.93e-5	3.04	2.37e-4	3.57
	1/28	141710	1.18e-5	3.16	1.36e-4	3.59
	1/32	184994	7.93e-6	3.00	8.56e-5	3.49
	1/36	234038	5.57e-6	3.00	5.68e-5	3.47
	1/48	415730	2.35e-6	2.99	2.11e-5	3.44
	1/64	738626	9.94e-7	3.00	7.86e-6	3.44
	1/96	1660898	2.95e-7	3.00	1.92e-6	3.48
	1/128	2951810	1.24e-7	3.00	7.03e-7	3.48

Table 6.2: Example 1, quasi-uniform scheme for the postprocessed unknowns.

k	h	N	$\mathtt{e}(\mathbf{t})$	$\mathtt{r}(\mathbf{t})$	$\mathtt{e}(\boldsymbol{\sigma})$	$\mathtt{r}(\boldsymbol{\sigma})$	$\mathtt{e}(\boldsymbol{\xi})$	$\mathtt{r}(\boldsymbol{\xi})$	$\mathtt{e}(\mathbf{t},\boldsymbol{\sigma},\boldsymbol{\xi})$	$\mathtt{r}(\mathbf{t},\boldsymbol{\sigma},\boldsymbol{\xi})$	$\mathtt{eff}(\boldsymbol{\theta})$
	1/16	7266	8.58e-0	−−	3.20e+01	−−	1.44e-0	−−	3.31e+01	−−	0.1686
	1/20	11322	6.72e-0	1.09	2.56e+01	0.99	7.33e-1	3.03	2.65e+01	1.00	0.1683
	1/24	16274	5.49e-0	1.11	2.14e+01	0.99	4.28e-1	2.95	2.21e+01	1.00	0.1681
	1/28	22122	4.63e-0	1.12	1.83e+01	1.00	2.77e-1	2.82	1.89e+01	1.00	0.1679
0	1/32	28866	3.98e-0	1.13	1.60e+01	1.00	1.94e-1	2.67	1.65e+01	1.00	0.1678
	1/36	36506	3.48e-0	1.13	1.43e+01	1.00	1.44e-1	2.52	1.47e+01	1.01	0.1677
	1/48	64802	2.50e-0	1.14	1.07e+01	1.00	7.57e-2	2.25	1.10e+01	1.01	0.1674
	1/64	115074	1.80e-0	1.16	8.03e-0	1.00	4.43e-2	1.86	8.23e-0	1.01	0.1671
	1/96	258626	1.12e-0	1.17	5.36e-0	1.00	2.42e-2	1.49	5.47e-0	1.01	0.1668
	1/128	459522	8.01e-1	1.16	4.02e-0	1.00	1.64e-2	1.35	4.10e-0	1.01	0.1666
	1/16	22722	2.08e-1	−−	1.21e-0	−−	2.04e-3	−−	1.22e-0	−−	0.1623
	1/20	35442	1.32e-1	2.04	7.75e-1	1.99	9.23e-4	3.55	7.86e-1	1.99	0.1624
	1/24	50978	9.13e-2	2.02	5.39e-1	1.99	4.80e-4	3.59	5.47e-1	1.99	0.1624
	1/28	69330	6.71e-2	2.00	3.97e-1	1.99	2.76e-4	3.57	4.02e-1	1.99	0.1624
1	1/32	90498	5.14e-2	1.99	3.04e-1	1.99	1.72e-4	3.53	3.08e-1	1.99	0.1625
	1/36	114482	4.06e-2	1.99	2.40e-1	2.00	1.14e-4	3.49	2.44e-1	2.00	0.1625
	1/48	203330	2.29e-2	1.99	1.35e-1	2.00	4.30e-5	3.40	1.37e-1	2.00	0.1625
	1/64	361218	1.29e-2	1.99	7.61e-2	2.00	1.68e-5	3.27	7.72e-2	2.00	0.1626
	1/96	812162	5.77e-3	1.99	3.39e-2	2.00	4.51e-6	3.24	3.44e-2	2.00	0.1625
	1/128	1443330	3.25e-3	1.99	1.91e-2	2.00	1.78e-6	3.24	1.93e-2	2.00	0.1626
	1/16	46370	4.69e-3	−−	3.33e-2	−−	1.38e-5	−−	3.36e-2	−−	0.1581
	1/20	72362	2.41e-3	2.98	1.71e-2	2.98	5.77e-6	3.89	1.73e-2	2.98	0.1580
	1/24	104114	1.40e-3	2.98	9.91e-3	2.99	2.83e-6	3.91	1.00e-2	2.99	0.1580
	1/28	141626	8.84e-4	2.99	6.25e-3	2.99	1.55e-6	3.92	6.31e-3	2.99	0.1580
2	1/32	184898	5.93e-4	2.99	4.19e-3	2.99	9.14e-7	3.93	4.23e-3	2.99	0.1580
	1/36	233930	4.17e-4	2.99	2.94e-3	3.00	5.75e-7	3.94	2.97e-3	3.00	0.1580
	1/48	415586	1.77e-4	2.99	1.24e-3	2.99	1.85e-7	3.94	1.26e-3	2.99	0.1580
	1/64	738434	7.47e-5	2.99	5.25e-4	3.00	5.94e-8	3.94	5.31e-4	3.00	0.1580
	1/96	1660610	2.22e-5	2.99	1.56e-4	3.00	1.20e-8	3.94	1.58e-4	3.00	0.1580
	1/128	2951426	9.39e-6	2.99	6.59e-5	3.00	3.86e-9	3.94	6.65e-5	3.00	0.1581

Table 6.3: Example 2, quasi-uniform scheme.

k	h	N	$\mathtt{e}(\mathbf{u})$	$\mathtt{r}(\mathbf{u})$	$\mathtt{e}(\mathtt{p})$	$\mathtt{r}(\mathtt{p})$
0	1/16	7266	1.24e-1	−−	3.90e-0	−−
	1/20	11322	8.19e-2	1.84	3.12e-0	1.01
	1/24	16274	5.93e-2	1.77	2.60e-0	1.01
	1/28	22122	4.58e-2	1.68	2.22e-0	1.01
	1/32	28866	3.71e-2	1.58	1.94e-0	1.00
	1/36	36506	3.11e-2	1.49	1.73e-0	1.00
	1/48	64802	2.12e-2	1.34	1.29e-0	1.00
	1/64	115074	1.51e-2	1.18	9.70e-1	1.00
	1/96	258626	9.54e-3	1.13	6.46e-1	1.00
	1/128	459522	6.77e-3	1.19	4.85e-1	1.00
1	1/16	22722	1.56e-3	−−	1.38e-1	−−
	1/20	35442	7.70e-4	3.17	8.87e-2	1.99
	1/24	50978	4.35e-4	3.14	6.17e-2	1.99
	1/28	69330	2.69e-4	3.10	4.54e-2	1.99
	1/32	90498	1.79e-4	3.08	3.48e-2	2.00
	1/36	114482	1.25e-4	3.06	2.75e-2	2.00
	1/48	203330	5.21e-5	3.03	1.55e-2	2.00
	1/64	361218	2.20e-5	3.00	8.71e-3	2.00
	1/96	812162	6.52e-6	3.00	3.87e-3	2.00
	1/128	1443330	2.75e-6	3.00	2.18e-3	2.00
2	1/16	46370	1.96e-5	−−	3.60e-3	−−
	1/20	72362	8.04e-6	4.00	1.84e-3	3.01
	1/24	104114	3.88e-6	4.00	1.06e-3	3.01
	1/28	141626	2.09e-6	4.00	6.67e-4	3.01
	1/32	184898	1.23e-6	3.96	4.46e-4	3.01
	1/36	233930	7.65e-7	4.05	3.13e-4	3.01
	1/48	415586	2.42e-7	4.01	1.32e-4	3.01
	1/64	738434	7.64e-8	4.00	5.54e-5	3.01
	1/96	1660610	1.51e-8	4.00	1.63e-5	3.01
	1/128	2951426	4.78e-9	4.00	6.86e-6	3.01

Table 6.4: Example 2, quasi-uniform scheme for the postprocessed unknowns.

k	h	N	$\mathtt{e}(\mathbf{t})$	$\mathtt{r}(\mathbf{t})$	$\mathtt{e}(\boldsymbol{\sigma})$	$\mathtt{r}(\boldsymbol{\sigma})$	$\mathtt{e}(\boldsymbol{\xi})$	$\mathtt{r}(\boldsymbol{\xi})$	$\mathtt{e}(\mathbf{t},\boldsymbol{\sigma},\boldsymbol{\xi})$	$\mathtt{r}(\mathbf{t},\boldsymbol{\sigma},\boldsymbol{\xi})$	$\mathtt{eff}(\boldsymbol{\theta})$
0	1/2	366	3.39e-0	−−	1.59e+01	−−	1.55e+01	−−	2.25e+01	−−	1.1530
	1/4	1402	2.15e-0	0.66	1.11e+01	0.52	6.37e-0	1.29	1.30e+01	0.79	1.0015
	1/6	3110	1.50e-0	0.90	8.70e-0	0.61	3.65e-0	1.37	9.55e-0	0.76	0.9548
	1/8	5490	1.12e-0	1.02	7.16e-0	0.68	2.25e-0	1.68	7.58e-0	0.80	0.9281
	1/10	8542	9.00e-1	0.96	6.05e-0	0.76	1.53e-0	1.74	6.30e-0	0.83	0.9170
	1/12	12266	7.70e-1	0.86	5.22e-0	0.80	1.15e-0	1.56	5.40e-0	0.84	0.9148
	1/14	16662	6.77e-1	0.83	4.59e-0	0.83	9.21e-1	1.45	4.73e-0	0.86	0.9151
	1/16	21730	6.01e-1	0.89	4.09e-0	0.86	7.50e-1	1.54	4.21e-0	0.88	0.9149
	1/18	27470	5.35e-1	0.98	3.69e-0	0.88	6.11e-1	1.74	3.78e-0	0.91	0.9137
	1/20	33882	4.78e-1	1.06	3.36e-0	0.90	4.97e-1	1.96	3.43e-0	0.93	0.9119
	1/40	134962	2.25e-1	1.09	1.75e-0	0.94	1.01e-1	2.29	1.76e-0	0.96	0.9056
	1/80	538722	1.11e-1	1.02	8.84e-1	0.98	2.28e-2	2.15	8.91e-1	0.99	0.9066
	1/160	2152642	5.53e-2	1.00	4.43e-1	1.00	5.51e-3	2.05	4.47e-1	1.00	0.9065
	1/200	3362802	4.42e-2	1.00	3.55e-1	1.00	3.51e-3	2.02	3.58e-1	1.00	0.9064
	1/220	4068682	4.02e-2	1.00	3.23e-1	1.00	2.90e-3	2.02	3.25e-1	1.00	0.9063
	1/240	4841762	3.68e-2	1.00	2.96e-1	1.00	2.43e-3	2.01	2.98e-1	1.00	0.9067
	1/300	7564202	2.95e-2	1.00	2.37e-1	1.00	1.55e-3	2.01	2.38e-1	1.00	0.9067
	1/400	13445602	2.21e-2	1.00	1.77e-1	1.00	8.70e-4	2.01	1.79e-1	1.00	0.9065
1	1/2	1114	1.51e-0	−−	7.34e-0	−−	5.12e-0	−−	9.08e-0	−−	0.8729
	1/4	4338	6.63e-1	1.18	3.84e-0	0.94	1.95e-0	1.39	4.35e-0	1.06	0.8278
	1/6	9674	4.50e-1	0.96	2.36e-0	1.20	1.16e-0	1.28	2.66e-0	1.21	0.8336
	1/8	17122	3.58e-1	0.79	1.60e-0	1.34	7.85e-1	1.35	1.82e-0	1.33	0.8606
	1/10	26682	2.57e-1	1.49	1.16e-0	1.45	5.02e-1	2.01	1.29e-0	1.54	0.8561
	1/12	38354	1.71e-1	2.24	8.75e-1	1.54	3.00e-1	2.81	9.40e-1	1.73	0.8281
	1/14	52138	1.12e-1	2.76	6.81e-1	1.62	1.76e-1	3.48	7.12e-1	1.80	0.8031
	1/16	68034	7.59e-2	2.89	5.44e-1	1.68	1.06e-1	3.75	5.59e-1	1.81	0.7919
	1/18	86042	5.59e-2	2.60	4.44e-1	1.72	7.17e-2	3.36	4.53e-1	1.79	0.7920
	1/20	106162	4.50e-2	2.06	3.69e-1	1.75	5.45e-2	2.61	3.76e-1	1.78	0.7979
	1/40	423522	1.19e-2	1.92	1.02e-1	1.85	9.66e-3	2.50	1.03e-1	1.86	0.8356
2	1/2	2246	7.37e-1	−−	3.52e-0	−−	2.42e-0	−−	4.33e-0	−−	0.6759
	1/4	8810	4.43e-1	0.73	1.34e-0	1.39	1.15e-0	1.07	1.82e-0	1.25	0.7723
	1/6	19694	2.98e-1	0.98	6.60e-1	1.75	6.33e-1	1.48	9.61e-1	1.58	0.8532
	1/8	34898	1.61e-1	2.15	3.73e-1	1.98	3.02e-1	2.57	5.06e-1	2.23	0.6371
	1/10	54422	8.71e-2	2.74	2.29e-1	2.19	1.44e-1	3.32	2.84e-1	2.59	0.5190
	1/12	78266	5.31e-2	2.72	1.50e-1	2.34	7.77e-2	3.38	1.77e-1	2.61	0.5272
	1/14	106430	3.45e-2	2.79	1.03e-1	2.43	4.66e-2	3.32	1.18e-1	2.62	0.5931

Table 6.5: Example 3, quasi-uniform scheme.

k	h	N	$\mathtt{e}(\mathbf{t})$	$\mathtt{r}(\mathbf{t})$	$\mathtt{e}(\boldsymbol{\sigma})$	$\mathtt{r}(\boldsymbol{\sigma})$	$\mathtt{e}(\boldsymbol{\xi})$	$\mathtt{r}(\boldsymbol{\xi})$	$\mathtt{e}(\mathbf{t},\boldsymbol{\sigma},\boldsymbol{\xi})$	$\mathtt{r}(\mathbf{t},\boldsymbol{\sigma},\boldsymbol{\xi})$	$\mathtt{eff}(\boldsymbol{\theta})$
	0.5000	366	3.39e-0	−−	1.59e+01	−−	1.55e+01	−−	2.25e+01	−−	1.1530
	0.5000	484	3.00e-0	0.88	1.52e+01	0.36	8.34e-0	4.45	1.76e+01	1.78	0.9389
	0.5000	674	2.48e-0	1.15	1.14e+01	1.74	7.01e-0	1.05	1.36e+01	1.55	0.9263
	0.5000	1032	1.90e-0	1.26	1.01e+01	0.57	3.88e-0	2.78	1.09e+01	1.01	0.8639
	0.5000	1396	1.59e-0	1.16	7.51e-0	1.93	3.61e-0	0.48	8.49e-0	1.68	0.8574
	0.5000	2138	1.24e-0	1.16	6.15e-0	0.94	1.77e-0	3.36	6.52e-0	1.24	0.8077
	0.5000	3506	9.55e-1	1.07	4.61e-0	1.16	1.38e-0	1.00	4.91e-0	1.15	0.8192
	0.2500	6558	6.93e-1	1.02	3.39e-0	0.98	9.43e-1	1.21	3.59e-0	1.00	0.8037
	0.2500	10426	5.35e-1	1.12	2.66e-0	1.05	3.67e-1	4.07	2.74e-0	1.17	0.7843
0	0.1768	17278	4.15e-1	1.00	2.02e-0	1.10	2.26e-1	1.92	2.07e-0	1.10	0.7757
	0.1250	33354	2.98e-1	1.00	1.42e-0	1.07	1.05e-1	2.32	1.45e-0	1.08	0.7645
	0.0884	59296	2.23e-1	1.01	1.04e-0	1.08	5.83e-2	2.06	1.06e-0	1.08	0.7579
	0.0625	103338	1.70e-1	0.99	7.91e-1	0.97	3.36e-2	1.98	8.10e-1	0.98	0.7555
	0.0625	177166	1.28e-1	1.04	5.91e-1	1.08	1.86e-2	2.19	6.05e-1	1.08	0.7519
	0.0442	324068	9.58e-2	0.97	4.44e-1	0.95	1.08e-2	1.81	4.54e-1	0.95	0.7552
	0.0313	559566	7.24e-2	1.02	3.35e-1	1.03	6.35e-3	1.94	3.43e-1	1.03	0.7560
	0.0221	859962	5.86e-2	0.98	2.71e-1	0.99	3.58e-3	2.66	2.77e-1	0.99	0.7550
	0.0156	1582206	4.37e-2	0.97	2.01e-1	0.98	2.38e-3	1.35	2.06e-1	0.98	0.7524
	0.0156	2413766	3.50e-2	1.05	1.58e-1	1.13	1.29e-3	2.88	1.62e-1	1.13	0.7481
	0.0110	4324014	2.65e-2	0.95	1.22e-1	0.89	7.59e-4	1.83	1.25e-1	0.90	0.7568
	0.5000	1114	1.51e-0	−−	7.34e-0	−−	5.12e-0	−−	9.08e-0	−−	0.8729
	0.5000	1322	9.65e-1	5.21	7.01e-0	0.54	2.19e-0	9.94	7.40e-0	2.38	0.7937
	0.5000	2058	7.06e-1	1.41	3.90e-0	2.64	2.10e-0	0.19	4.49e-0	2.26	0.7891
	0.5000	2546	5.16e-1	2.95	3.61e-0	0.72	1.11e-0	6.02	3.81e-0	1.53	0.7893
	0.5000	4162	4.18e-1	0.86	1.67e-0	3.14	1.08e-0	0.09	2.03e-0	2.56	0.7705
1	0.5000	4626	1.91e-1	14.85	1.59e-0	0.94	1.68e-1	35.21	1.61e-0	4.41	0.7206
	0.5000	7098	1.35e-1	1.61	1.00e-0	2.16	1.66e-1	0.07	1.03e-0	2.11	0.7158
	0.5000	11198	8.37e-2	2.10	6.14e-1	2.15	1.15e-1	1.62	6.30e-1	2.14	0.7141
	0.3536	17566	5.41e-2	1.94	3.72e-1	2.22	6.04e-2	2.84	3.81e-1	2.24	0.6854
	0.2500	27334	3.47e-2	2.01	2.25e-1	2.27	2.55e-2	3.90	2.29e-1	2.29	0.6636
	0.2500	41090	2.17e-2	2.30	1.47e-1	2.10	1.59e-2	2.32	1.49e-1	2.11	0.6543
	0.1768	59146	1.42e-2	2.35	1.11e-1	1.56	7.09e-3	4.45	1.12e-1	1.59	0.7023
	0.5000	2246	7.37e-1	−−	3.52e-0	−−	2.42e-0	−−	4.33e-0	−−	0.6759
	0.5000	2552	4.95e-1	6.22	3.06e-0	2.18	1.15e-0	11.65	3.31e-0	4.23	0.6437
	0.5000	4106	4.51e-1	0.40	2.04e-0	1.70	1.16e-0	-0.03	2.39e-0	1.36	0.7652
	0.5000	4718	1.73e-1	13.76	1.15e-0	8.25	3.06e-1	19.15	1.20e-0	9.87	0.6242
2	0.5000	5936	1.73e-1	0.03	1.11e-0	0.32	3.13e-1	-0.20	1.17e-0	0.28	0.7404
	0.5000	8810	4.63e-2	6.66	3.49e-1	5.86	8.74e-2	6.46	3.63e-1	5.91	0.6054
	0.5000	9992	3.33e-2	5.23	3.36e-1	0.59	3.27e-2	15.63	3.40e-1	1.05	0.7023
	0.5000	15290	2.17e-2	2.02	1.55e-1	3.65	2.49e-2	1.29	1.58e-1	3.59	0.6374
	0.5000	20648	1.02e-2	5.03	8.33e-2	4.12	1.16e-2	5.05	8.48e-2	4.15	0.5758

Table 6.6: Example 3, adaptive scheme.

k	h	N	$\mathtt{e}(\mathbf{t})$	$\mathtt{r}(\mathbf{t})$	$\mathtt{e}(\boldsymbol{\sigma})$	$\mathtt{r}(\boldsymbol{\sigma})$	$\mathtt{e}(\boldsymbol{\xi})$	$\mathtt{r}(\boldsymbol{\xi})$	$\mathtt{e}(\mathbf{t},\boldsymbol{\sigma},\boldsymbol{\xi})$	$\mathtt{r}(\mathbf{t},\boldsymbol{\sigma},\boldsymbol{\xi})$	$\mathtt{eff}(\boldsymbol{\theta})$
	0.3750	724	1.40e-0	−−	7.46e-0	−−	6.08e-0	−−	9.73e-0	−−	1.7390
	0.1875	2790	8.60e-1	0.70	4.68e-0	0.67	2.57e-0	1.24	5.41e-0	0.85	1.7570
	0.1250	6200	6.18e-1	0.82	3.43e-0	0.77	1.69e-0	1.04	3.87e-0	0.82	1.7718
	0.0938	10954	4.64e-1	1.00	2.73e-0	0.79	1.14e-0	1.34	3.00e-0	0.89	1.7505
	0.0750	17052	3.65e-1	1.07	2.27e-0	0.83	8.01e-1	1.60	2.44e-0	0.93	1.7282
0	0.0625	24494	3.02e-1	1.05	1.94e-0	0.88	5.82e-1	1.75	2.04e-0	0.96	1.7154
	0.0536	33280	2.59e-1	1.00	1.68e-0	0.92	4.45e-1	1.75	1.76e-0	0.98	1.7116
	0.0469	43410	2.28e-1	0.96	1.48e-0	0.95	3.57e-1	1.64	1.54e-0	0.99	1.7126
	0.0417	54884	2.04e-1	0.94	1.32e-0	0.96	2.98e-1	1.53	1.37e-0	0.99	1.7146
	0.0375	67702	1.85e-1	0.94	1.19e-0	0.97	2.55e-1	1.48	1.23e-0	0.99	1.7150
	0.0188	269802	8.70e-2	1.09	6.05e-1	0.98	6.44e-2	1.99	6.14e-1	1.01	1.6799
	0.0094	1077202	4.12e-2	1.08	3.03e-1	1.00	1.34e-2	2.26	3.06e-1	1.00	1.7048
	0.3750	2214	5.81e-1	−−	3.15e-0	−−	2.18e-0	−−	3.87e-0	−−	1.6991
	0.1875	8650	2.96e-1	0.97	1.56e-0	1.02	9.92e-1	1.14	1.87e-0	1.05	1.5416
	0.1250	19310	1.87e-1	1.12	9.19e-1	1.30	5.55e-1	1.43	1.09e-0	1.33	1.3667
	0.0938	34194	1.44e-1	0.91	5.84e-1	1.58	3.76e-1	1.35	7.09e-1	1.49	1.3268
1	0.0750	53302	1.16e-1	0.97	3.93e-1	1.77	2.76e-1	1.39	4.95e-1	1.62	1.3085
	0.0625	76634	9.21e-2	1.27	2.82e-1	1.82	2.02e-1	1.72	3.59e-1	1.76	1.2165
	0.0536	104190	7.09e-2	1.70	2.13e-1	1.85	1.43e-1	2.22	2.66e-1	1.95	1.0810
	0.0469	135970	5.31e-2	2.16	1.66e-1	1.86	9.95e-2	2.73	2.00e-1	2.11	0.9717
	0.0417	171974	3.94e-2	2.54	1.33e-1	1.88	6.90e-2	3.11	1.55e-1	2.19	0.9067
	0.3750	4472	3.23e-1	−−	1.69e-0	−−	1.17e-0	−−	2.08e-0	−−	1.1581
	0.1875	17582	1.74e-1	0.89	7.14e-1	1.25	5.10e-1	1.19	8.95e-1	1.22	1.0612
2	0.1250	39332	1.31e-1	0.69	3.17e-1	2.01	3.24e-1	1.12	4.71e-1	1.58	1.1396
	0.0938	69722	9.33e-2	1.19	1.65e-1	2.27	2.05e-1	1.60	2.79e-1	1.83	0.9407
	0.0750	108752	6.23e-2	1.81	1.00e-1	2.22	1.22e-1	2.31	1.70e-1	2.22	0.7126
	0.0625	156422	4.04e-2	2.38	6.30e-2	2.55	7.23e-2	2.88	1.04e-1	2.69	0.5927

Table 6.7: Example 4, quasi-uniform scheme.

k	h	N	$\mathtt{e}(\mathbf{t})$	$\mathtt{r}(\mathbf{t})$	$\mathtt{e}(\boldsymbol{\sigma})$	$\mathtt{r}(\boldsymbol{\sigma})$	$\mathtt{e}(\boldsymbol{\xi})$	$\mathtt{r}(\boldsymbol{\xi})$	$\mathtt{e}(\mathbf{t},\boldsymbol{\sigma},\boldsymbol{\xi})$	$\mathtt{r}(\mathbf{t},\boldsymbol{\sigma},\boldsymbol{\xi})$	$\mathtt{eff}(\boldsymbol{\theta})$
	0.3750	724	1.40e-0	−−	7.46e-0	−−	6.08e-0	−−	9.73e-0	−−	1.7390
	0.3750	942	1.17e-0	1.37	6.65e-0	0.88	3.21e-0	4.86	7.47e-0	2.00	1.5176
	0.3750	1334	1.02e-0	0.81	4.91e-0	1.74	2.93e-0	0.51	5.81e-0	1.45	1.4362
	0.2500	2414	7.23e-1	1.15	4.09e-0	0.61	1.56e-0	2.13	4.44e-0	0.91	1.4099
	0.2500	3324	6.09e-1	1.08	3.01e-0	1.92	1.42e-0	0.59	3.38e-0	1.70	1.3028
	0.1875	4516	4.87e-1	1.46	2.49e-0	1.24	7.03e-1	4.58	2.63e-0	1.64	1.1800
	0.1875	6676	3.94e-1	1.09	2.02e-0	1.07	5.18e-1	1.56	2.12e-0	1.10	1.1806
	0.1250	11264	2.93e-1	1.12	1.58e-0	0.95	2.67e-1	2.53	1.62e-0	1.02	1.1825
0	0.1250	16740	2.47e-1	0.86	1.25e-0	1.17	1.73e-1	2.21	1.29e-0	1.18	1.1262
	0.1250	27176	1.86e-1	1.17	9.96e-1	0.93	9.37e-2	2.52	1.02e-0	0.96	1.1629
	0.0884	41338	1.51e-1	1.02	7.97e-1	1.06	6.74e-2	1.57	8.14e-1	1.07	1.1508
	0.0625	69714	1.18e-1	0.92	6.13e-1	1.01	3.47e-2	2.54	6.25e-1	1.01	1.1347
	0.0625	110000	9.18e-2	1.11	4.84e-1	1.04	2.19e-2	2.02	4.93e-1	1.04	1.1440
	0.0442	168592	7.39e-2	1.02	3.95e-1	0.95	1.60e-2	1.47	4.02e-1	0.96	1.1607
	0.0442	232804	6.39e-2	0.91	3.39e-1	0.95	9.24e-3	3.41	3.45e-1	0.95	1.1568
	0.0313	372780	5.00e-2	1.04	2.67e-1	1.02	6.48e-3	1.51	2.71e-1	1.02	1.1598
	0.0313	542152	4.14e-2	1.02	2.20e-1	1.02	4.46e-3	1.99	2.24e-1	1.02	1.1673
	0.3750	2214	5.81e-1	−−	3.15e-0	−−	2.18e-0	−−	3.87e-0	−−	1.6991
	0.3750	2518	3.58e-1	7.51	2.61e-0	2.89	1.02e-0	11.81	2.83e-0	4.89	1.4725
	0.3750	3150	3.09e-1	1.33	1.63e-0	4.21	1.03e-0	-0.10	1.95e-0	3.30	1.3267
	0.3750	3798	1.93e-1	5.02	1.23e-0	2.99	4.82e-1	8.13	1.34e-0	4.05	1.1749
1	0.3750	5090	1.69e-1	0.90	8.04e-1	2.91	4.84e-1	-0.03	9.54e-1	2.30	1.2067
	0.3750	5490	8.81e-2	17.27	6.98e-1	3.75	1.13e-1	38.54	7.12e-1	7.72	1.1211
	0.3750	7706	7.38e-2	1.05	3.88e-1	3.46	1.11e-1	0.10	4.10e-1	3.26	0.8694
	0.2500	10582	4.30e-2	3.41	3.31e-1	1.00	4.99e-2	5.03	3.37e-1	1.23	1.0209
	0.2500	18142	2.62e-2	1.83	1.56e-1	2.79	4.16e-2	0.67	1.64e-1	2.68	0.8562
	0.3750	4472	3.23e-1	−−	1.69e-0	−−	1.17e-0	−−	2.08e-0	−−	1.1581
	0.3750	4880	1.86e-1	12.70	1.19e-0	8.03	4.98e-1	19.48	1.31e-0	10.67	0.9807
	0.3750	6062	1.77e-1	0.45	8.94e-1	2.66	5.10e-1	-0.23	1.04e-0	2.06	1.0595
2	0.3750	6830	9.99e-2	9.56	6.44e-1	5.50	2.02e-1	15.57	6.82e-1	7.14	0.9906
	0.3750	9104	9.37e-2	0.44	2.37e-1	6.97	2.05e-1	-0.10	3.27e-1	5.13	0.8652
	0.3750	9512	2.38e-2	62.55	1.88e-1	10.41	3.21e-2	84.45	1.93e-1	24.09	0.7652
	0.3750	11786	2.21e-2	0.68	1.78e-1	0.54	3.27e-2	-0.17	1.82e-1	0.52	0.9934

Table 6.8: Example 4, adaptive scheme.

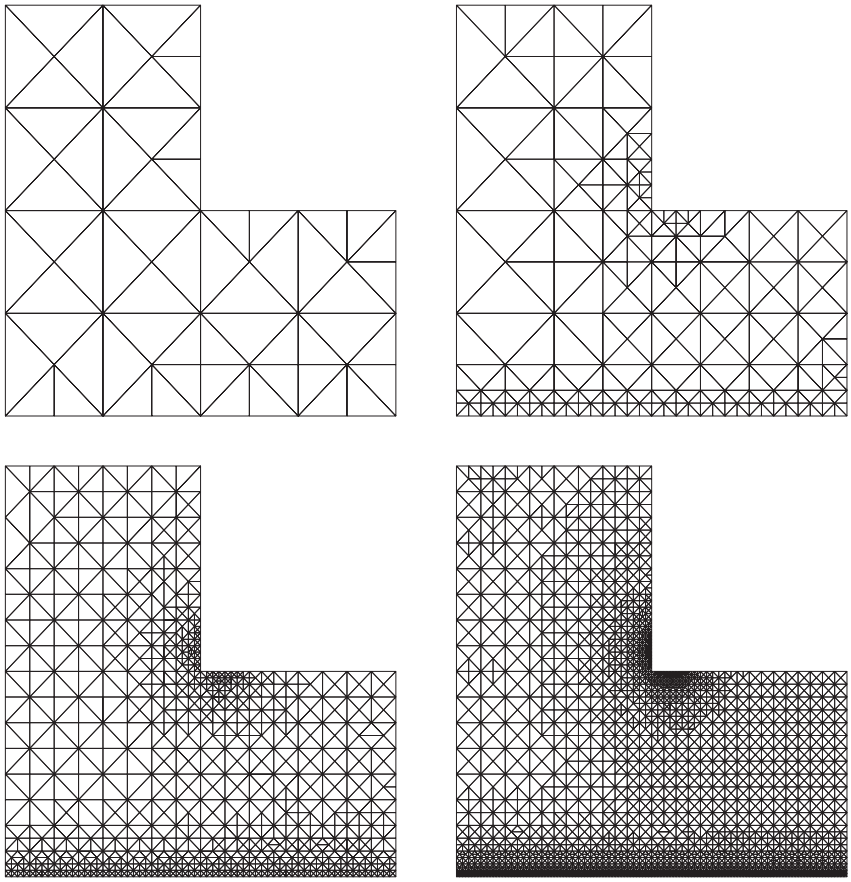

Figure 6.2: Example 3, adapted meshes for $k = 0$ with 484, 2138, 10426, and 33354 degrees of freedom.

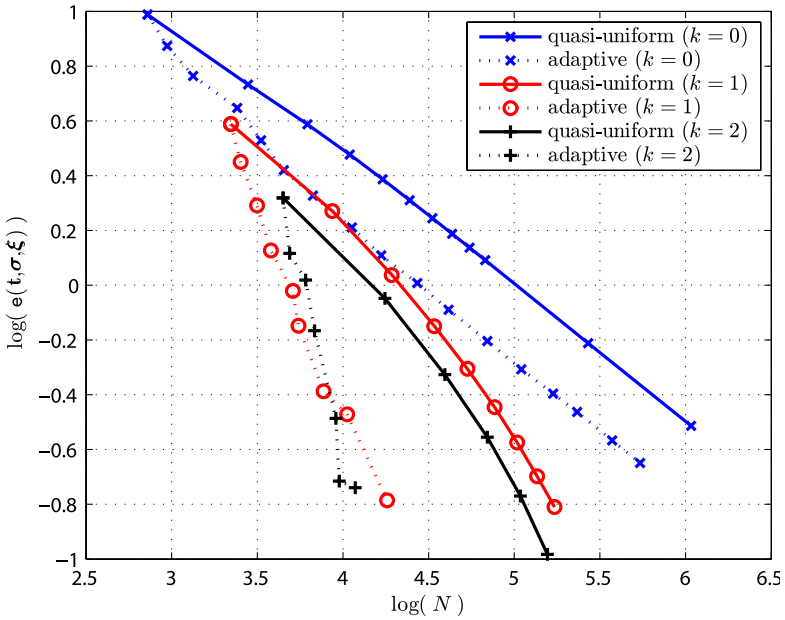

Figure 6.3: Example 4, $\mathsf{e}(\mathbf{t}, \boldsymbol{\sigma}, \boldsymbol{\xi})$ vs. N.

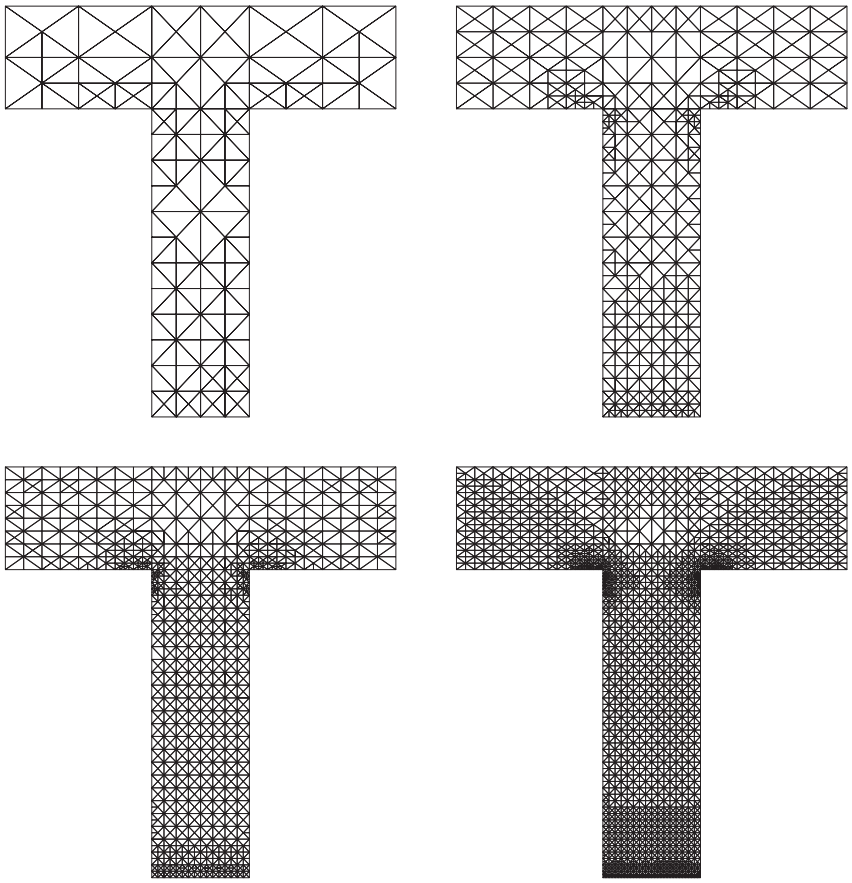

Figure 6.4: Example 4, adapted meshes for $k = 0$ with 1334, 4516, 11264, and 27176 degrees of freedom.

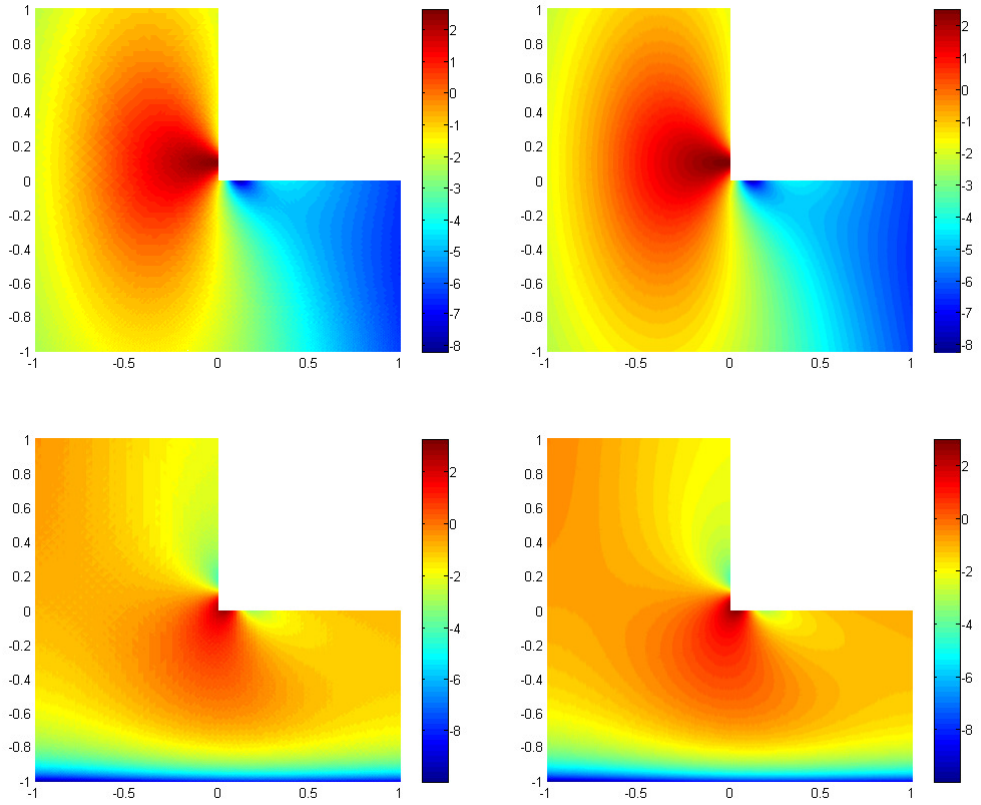

Figure 6.5: Example 3, approximate and exact σ_{21} and σ_{22} ($k = 0$ and $N = 177166$) for adaptive scheme.

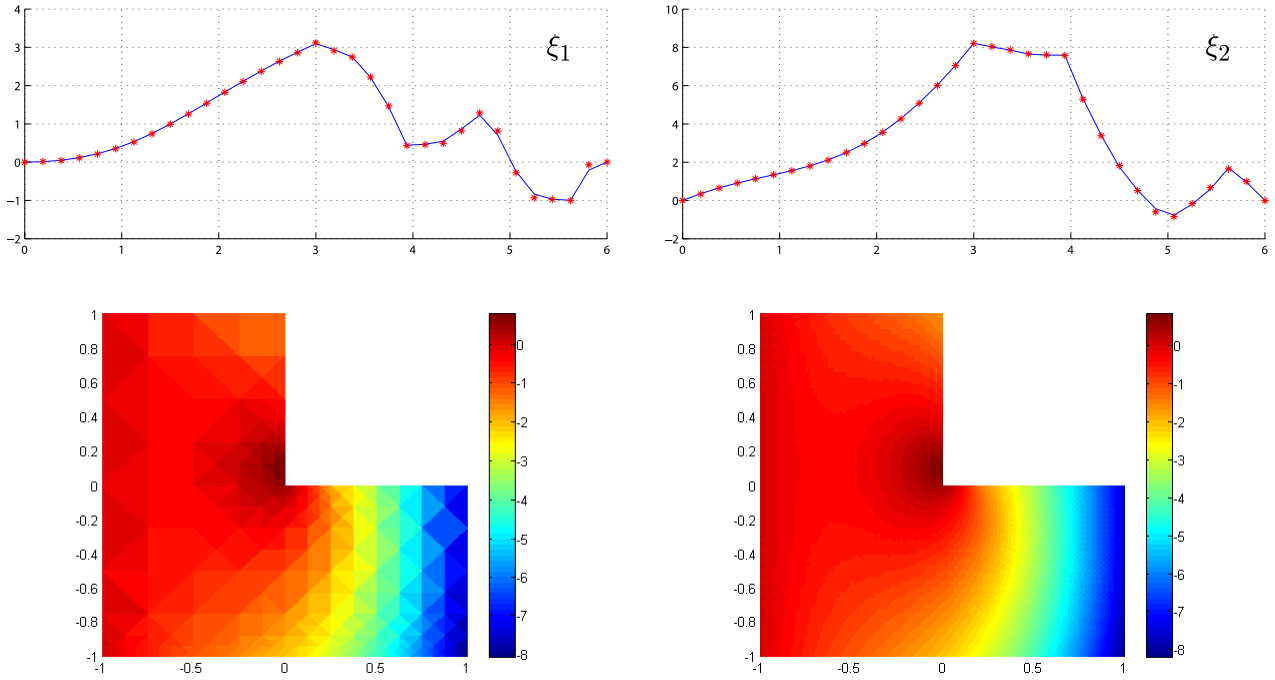

Figure 6.6: Example 3, approximate and exact $\boldsymbol{\xi}$ and u_2 ($k = 0$ and $N = 3506, 177166$) for adaptive scheme.

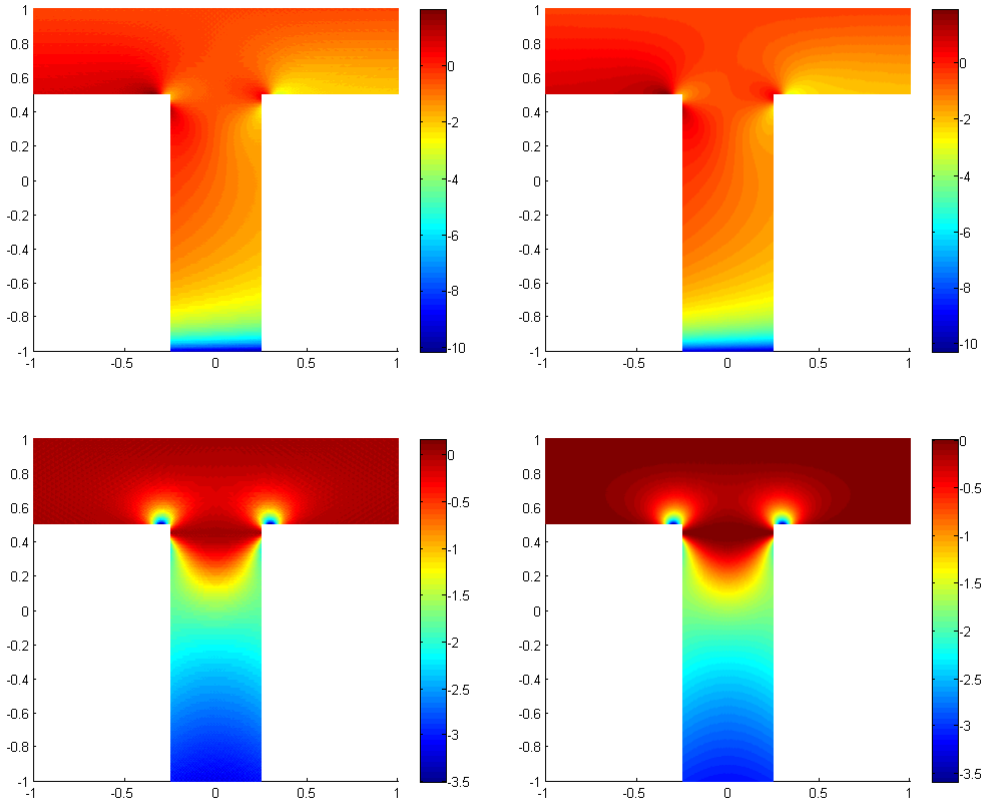

Figure 6.7: Example 4, approximate and exact σ_{11} and σ_{21} ($k = 0$ and $N = 168592$) for adaptive scheme.

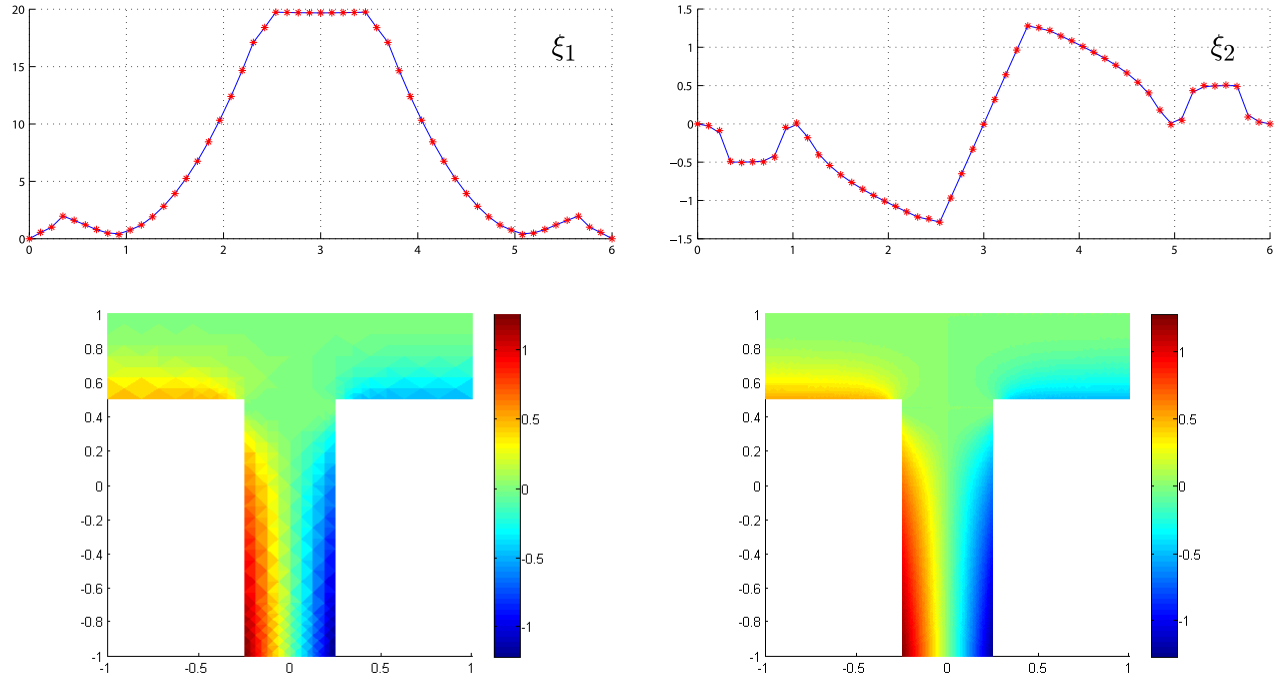

Figure 6.8: Example 4, approximate and exact $\boldsymbol{\xi}$ and u_2 ($k = 0$ and $N = 6676, 168592$) for adaptive scheme.

References

[1] D. N. Arnold, J. Douglas, and C. P. Gupta, *A family of higher order mixed finite element methods for plane elasticity*, Numer. Math., 45 (1984), pp. 1–22.

[2] F. Brezzi and M. Fortin, *Mixed and Hybrid Finite Element Methods*, Springer Verlag, 1991.

[3] E. Burman and P. Hansbo, *A unified stabilized method for Stokes' and Darcy's equations*, Journal of Computational and Applied Mathematics, 198 (2007), pp. 35–51.

[4] P. G. Ciarlet, *The Finite Element Method for Elliptic Problems*, Nort-Holland, 1978.

[5] P. Clément, *Approximation by finite element functions using local regularisation*, RAIRO Model. Math. et Anal. Numer., 9 (1975), pp. 77–84.

[6] A. I. Garralda-Guillem, G. N. Gatica, A. Márquez, and M. Ruiz-Galán, *A posteriori error analysis of twofold saddle point variational formulations for nonlinear boundary value problems*, IMA Journal of Numerical Analysis, 34 (2014), pp. 326–361.

[7] G. N. Gatica, *Solvability and Galerkin approximations of a class of nonlinear operator equations*, Zeitschrift für Analysis und ihre Anwendungen, 21 (2002), pp. 761–781.

[8] ——, *Analysis of a new augmented mixed finite element method for linear elasticity allowing* $\mathbb{RT}_0 - \mathbb{P}_1 - \mathbb{P}_0$ *approximations*, ESAIM Math. Model. Numer. Anal., 40 (2006), pp. 1–28.

[9] G. N. Gatica, L. F. Gatica, and A. Márquez, *Analysis of a pseudostress-based mixed finite element method for the Brinkman model of porous media flow*, Numerische Mathematik, 126 (2014), pp. 635–677.

[10] G. N. Gatica, M. González, and S. Meddahi, *A low-order mixed finite element method for a class of quasi-Newtonian Stokes flows. I: a priori error analysis*, Comput. Methods Appl. Mech. Engrg., 193 (2004), pp. 881–892.

[11] G. N. Gatica, N. Heuer, and S. Meddahi, *On the numerical analysis of nonlinear twofold saddle point problems*, IMA J. Numer. Anal., 23 (2003), pp. 301–330.

[12] G. N. Gatica, A. Márquez, and M. A. Sánchez, *Analysis of a velocity-pressure-pseudostress formulation for the stationary Stokes equations*, Comput. Methods Appl. Mech. Engrg., 199 (2010), pp. 1064–1079.

[13] ——, *A priori and a posteriori error analyses of a velocity-pseudostress formulation for a class of quasi-Newtonian Stokes flows*, Comput. Methods Appl. Mech. Engrg., 200 (2011), pp. 1619–1636.

[14] P. Hansbo and M. Juntunen, *Weakly imposed dirichlet boundary conditions for the Brinkman model of porous media flow*, Applied Numerical Mathematics, 59 (2009), pp. 1274–1289.

[15] R. Hiptmair, *Finite elements in computational electromagnetism*, Acta Numerica, 11 (2002), pp. 237–339.

[16] J. S. Howell, *Dual-mixed finite element approximation of Stokes and nonlinear Stokes problems using trace-free velocity gradients*, J. Comput. Appl. Math., 231 (2009), pp. 780–792.

[17] M. Juntunen and R. Stenberg, *Analysis of finite element methods for the Brinkman problem*, Calcolo, 47 (2010), pp. 129–147.

[18] A. F. D. Loula and J. N. C. Guerreiro, *Finite element analysis of nonlinear creeping flows*, Comput. Methods Appl. Mech. Engrg., 99 (1990), pp. 87–109.

[19] W. McLean, *Strongly Elliptic Systems and Boundary Integral Equations*, Cambridge University Press, London, 2000.

[20] A. Quarteroni and A. Valli, *Numerical Approximation of Partial Differential Equations*, Springer, Heidelberg, 1996.

[21] J. E. Roberts and J. M. Thomas, *Mixed and Hybrid Methods. In Handbook of Numerical Analysis, edited by P.G. Ciarlet and J.L. Lions, vol. II, Finite Element Methods (Part 1)*, Nort-Holland, Amsterdam, 1991.

[22] D. Sandri, *Sur l'approximation numérique des écoulements quasi-Newtoniens dont la viscosité suit la loi puissance ou la loi de Carreau*, Math. Model. Numer. Anal., 27 (1993), pp. 131–155.

[23] B. Scheurer, *Existence et approximation de point selles pour certain problemes non linéaires*, R.A.I.R.O. Analyse Numérique, 11 (1977), pp. 369–400.

[24] R. Verfürth, *A Review of A Posteriori Error Estimation and Adaptive-Mesh-Refinement Techniques*, Wiley, Chichester, 1996.